

HYDROMAGNETIC MIXED CONVECTIVE HEAT AND MASS TRANSFER THROUGH A POROUS MEDIUM IN A CYLINDRICAL ANNULUS WITH HEAT SOURCE/SINK

B. Ramakrishna Reddy

Department of Mathematics, Gokaraju Rangaraju Institute of Engineering and Technology, Hyderabad, India

Abstract

We analyze the Soret effect on mixed convective heat and mass transfer through a porous medium confined in a cylindrical annulus under a radial magnetic field. Two cases have been discussed by considering constant heat source/sink and heat generating sources in the energy equation. We also take the dissipative effects into account. The equations governing the flow, heat and mass transfer have been solved by a perturbation technique. The Soret effect and the dissipative effect on the velocity, temperature and concentration have been depicted through various profiles. The shear stress, the rate of heat and mass transfer have been evaluated numerically for variations in the parameters G , D^{-1} , R , N , Sc and So .

Keywords

MHD, Mixed Convection, Cylindrical Annulus, Heat Source/Sink, Porous Medium.

1 Introduction

The increasing cost of energy has lead technologists to examine measures which could considerably reduce the usage of the natural source energy (fossile). Thermal insulations will continue to find increased use as engineers seek to reduce cost. Heat transfer in porous thermal insulation with in vertical cylindrical annuli provide us insight into the mechanism of energy transport and enable engineers to use insulation more efficiently. In particular design engineers require relationships between heat transfer, geometry and boundary conditions which can be utilized cost-benefit analysis to determine the amount of insulation that will yield the maximum investment. Apart from this, the study of flow and heat transfer in the annular region between the concentric cylinders has applications in nuclear waste disposal research. It is known that canisters filled with radio active rays be buried in the earth so as to isolate them from human population and is of interest to determine the surface temperature of these canisters. This surface temperature strongly depends on the buoyancy driven flow sustained by the heated surface and the possible moment of ground water past it. This phenomenon make idealized to the study of convection flow in a porous medium contained in a cylindrical annulus and extensively has been made on these lines (15,16,17). Free convection in a vertical porous annulus has been extensively studied by Prasad (15), Prasad and Kulacki (16) and Prasad et al (17) both theoretically and experimentally. Caltagirone (3) has published a detailed theoretical study of free convection in a horizontal porous annulus, including possible three dimensional and transient effects. Similar studies for fluid filled annuli are available in the literature (20). Convection through annular regions under steady state conditions has also been discussed with the two cylindrical surfaces kept at different temperatures (8). This work has been extended in temperature dependent convection flow (5,7,8) as well as convection flows through horizontal porous channel whose inner surface is maintained at constant temperature, while the other surface is maintained at circumferentially varying sinusoidal temperature (11,21,28). Free convection flow and heat transfer in hydro magnetic case is important in nuclear and space technology (8,12,14,24,30,31). In particular such convection flow in a vertical annulus region in the presence of radial magnetic field has been investigated by Sastry and Bhadram(22). Nanda and Purushotham (9) have analyzed the free convection of a thermal conducting viscous incompressible fluid induced by a traveling thermal waves on the circumference of a long vertical circular cylindrical pipe. The solutions of the velocity and temperature fields are obtained using the long wave approximations. Ganapathi and Purushotham (6) have studied the unsteady flow induced by a traveling thermal wave imposed on the circumference of a long vertical cylindrical column of a fluid in a saturated porous medium. The analysis is carried out following White head (29), Neeraja(10) has made a study of the fluid flow and heat transfer in a viscous incompressible fluid confined in an annulus bounded by two rigid cylinders. The flow is generated by periodic traveling waves imposed on the outer cylinder and the inner cylinder is maintained at constant temperature. Chen and Yuh (4) have investigated the heat and mass transfer characteristics of natural convection flow along a vertical cylinder under the combined buoyancy effects of thermal and species diffusion. The analysis is restricted to processes in which the diffusion-thermo and thermo-diffusion effects as well as the inter facial velocities from species diffusion are negligible. The surface of the cylinder is either maintained at a uniform temperature and concentration (or) subjected to uniform heat and mass

flux. The conservation equations of the laminar boundary layer are solved in finite difference method. Sivanjaneya Prasad (25) has investigated the free convection flow of an incompressible, viscous fluid through a porous medium in the annulus between the porous concentric cylinders under the influence of a radial magnetic field. Antonio (2) has investigated the laminar flow, heat transfer in a vertical cylindrical duct by taking in to account both viscous dissipation and the effect of buoyancy. The limiting case of fully developed natural convection in porous annuli is solved analytically for steady and transient cases by E.Shaarawi and AL – Nimr (23) and AL – Nimr (1). Philip (13) has obtained analytical solution for the annular porous media valid for low modified Reynolds number. Rani (19) has analyzed the unsteady convection heat and mass transfer through a cylindrical annulus with constant heat sources taking the aspect ratio ' δ ' as perturbation parameter. The governing equations have been solved by a regular perturbation method. The effect of the traveling transverse wave imposed on the boundary of the cylinders on the velocity, temperature and concentration have been discussed in detail. Srevani (27) has investigated the convective heat and mass transfer through a porous medium in a cylindrical annulus under radial magnetic field and with sores effect. Taking G/R much less than 1 the coupled equations governing the flow, heat and mass transfer have been solved by regular perturbation method. Prasad (18) has analyzed the convective heat and mass transfer through a porous cylindrical annulus in the presence of heat generating source under radial magnetic field (assuming the Eckert number Ec much less than 1). The governing equations have been solved by regular perturbation method. Recently Srenivas Reddy(26) has discussed the sores effect on mixed convective heat and mass transfer through a porous cylindrical annulus. The expression for the velocity, temperature and concentration have been analyzed computationally for different parameters.

2. Formulation and solution

We consider the fully developed, steady laminar free convective flow of an incompressible, viscous, electrically conducting fluid through a porous medium in a annular region between two vertical co-axial circular pipes. We choose the cylindrical polar coordinates system $0(r, \theta, z)$ with the inner and outer cylinders at $r=a$ and $r=b$ respectively. The fluid is subjected to the influence of a radial magnetic field (H_0/r) . Pipes being sufficiently long all the physical quantities are independent of the axial coordinate z . The fluid is chosen to be of small conductivity so that the Magnetic Reynolds number is much smaller than unity and hence the induced magnetic field is negligible compared to the applied radial field. Also the motion being rotationally symmetric the azimuthally velocity V is zero. The equation of motion governing the MHD flow through the porous medium are

$$u_r + u/r = 0 \quad (2.1)$$

$$\rho_e u u_r = -p_r + \mu(u_{rr} + u_r/r - u/r^2) - (\mu/k)u \quad (2.2)$$

$$\rho_e u w_r = -p_z + \mu(w_{rr} + w_r/r - (\mu/k)w - \rho g - (\sigma \mu_e^2 H_0^2 a^2 / r^2)w) \quad (2.3)$$

$$u C_r = D(C_{rr} + C_r/r) + k_{11}(Tr_r + Tr/r) \quad (2.4)$$

$$\rho = \rho_e(1 - \beta(T - T_0) - \beta^*(C - C_e)) \quad (2.5)$$

where (u, w) are the velocity components along $0(r, z)$ directions respectively, ρ is the density of the fluid, p is the pressure, T, C are the temperature and Concentration, μ is the coefficient of viscosity, C_p is the specific heat at constant pressure, k is the porous permeability, σ is the electrically conductivity, μ_e is the magnetic permeability and ρ_e, T_e, C_e are density, temperature and Concentration in the equilibrium state, β^* is the volumetric coefficient of expansion with mass fraction, D_1 is the molecular diffusivity and k_{11} is the cross diffusivity (suffices r and z indicate differentiation w.r.t. the variables).

The boundary conditions are

$$w(a) = w(b) = 0 \quad (2.6)$$

$$C(a) = C_i, \quad C(b) = C_o \quad (2.7)$$

In the hydrostatic state equation (2.3) gives

$$-\rho_e g - p_{e,z} = 0 \quad (2.8)$$

where ρ_e and p_e are the density and pressure in the static case and hence

$$-\rho g - p_z = -(\rho - \rho_e)g - p_{d,z} \quad (2.9)$$

where p_d is the dynamic pressure

Also substituting (2.8) in (2.2) we find

$$\frac{\partial p_d}{\partial r} = f(r)$$

Using the relation (2.6) – (2.9) in (2.1) – (2.5) the equations governing free convection Heat and mass transfer flow under no pressure gradient are

$$w_{rr} + w_r/r - (\beta g/\nu)(T - T_e) - (w/r^2) - (w/k) = 0 \quad (2.10)$$

$$C_{rr} + C_r/r = -(ScS_0/N)(\theta_{rr} + \theta_r/r) \quad (2.11)$$

3. Case when heat source is constant

The equation of energy for the constant heat source is

$$\rho C_p (uT_r) = k_1(T_{rr} + T_r/r) + \mu(2(u_r^2 + u^2/r^2) + w_r^2) + (\mu/k + \sigma\mu_e^2 H_o^2)(u^2 + w^2) + Q \quad (3.1)$$

where k_1 is the coefficient of thermal conductivity and Q is the strength of the heat source/sink. Making use of (2.7) in (3.1) the above energy equation reduces to

$$T_{rr} + (1 - au_a/\nu)T_r/r + \mu(2(u^2/r^2) + w_r^2) + (\mu/k + \sigma\mu_e^2 H_o^2)(u^2 + w^2) + Q = 0 \quad (3.2)$$

The boundary conditions related to the temperature are

$$T(a) = T_i \text{ and } T(b) = T_0 \quad (3.3)$$

$$C(a) = C_i \text{ and } C(b) = C_0$$

Introducing the non-dimensional variables

$$(r', w') \text{ as } r' = r/a, w' = w(a/\nu) \quad (3.4)$$

$$\theta = \frac{T - T_e}{T_i - T_e}, \quad C' = \frac{C - C_e}{C_i - C_e}$$

the equations (2.9), (2.10) and (3.2) reduce to

$$w_{rr} + (1/r)w_r - (D_2^{-1} + (M^2/r^2))w = -G\theta \quad (3.5)$$

$$\theta_{rr} + \theta_r/r = -PE_c(w_r^2 + \lambda^2/r^4) + \alpha \quad (3.6)$$

$$C_{rr} + (1/r)C_r = -(ScS_0/N)(\theta_{rr} + (1/r)\theta_r) \quad (3.7)$$

where $M = (\sigma\mu_e^2 H_o^2 a^2 / \rho\nu)^{1/2}$ (the Hartmann number)

$G = (\beta g a^3 (T_i - T_e) / \nu^2)$ (the Grashoff number) $D_2^{-1} = (a^2/k)$ (the Darcy parameter)

$P = (\mu C_p / k_1)$ (the Prandtl number) $E_e = (\nu / k_1 a^2 (T_i - T_e))$ (the Eckert number)

$$\alpha = \frac{QL^2}{k_1} \text{ (the Heat Source parameter)} \quad Sc = \frac{\nu}{D_1} \text{ (the Schmidt number)}$$

$$N = \frac{\beta^*(C_i - C_o)}{\beta(T_i - T_o)} \text{ (the buoyancy ratio)} \quad So = \frac{k_{11}\beta^*}{\beta\nu} \text{ (the Soret parameter)}$$

The corresponding boundary conditions are

$$w = 0, \theta = 1, C = 1 \text{ on } r = 1$$

$$w = 0, \theta = m_1, C = m_2 \text{ on } r = s \quad (3.7)$$

where

$$m_1 = \frac{T_o - T_e}{T_i - T_e}, \quad m_2 = \frac{C_o - C_e}{C_i - C_e}$$

Assuming $Ec \ll 1$, we take the solution as

$$w = w_0 + Ec w_1 + \dots$$

$$\theta = \theta_0 + Ec \theta_1 + \dots \quad (3.8)$$

$$C = C_0 + Ec C_1 + \dots$$

Substituting (3.8) in equations (3.5) -(3.7) and separating the like powers of Ec

The equations to the zeroth order are

$$w_{0,rr} + (1/r)w_{0,r} - (D_2^{-1} + \frac{M^2}{r^2})w_0 = -G\theta_0 \quad (3.9)$$

$$\theta_{0,rr} + (1/r)\theta_{0,r} + \alpha = 0 \quad (3.10)$$

$$C_{0,rr} + (1/r)C_{0,r} = -(\frac{ScSo}{N})(\theta_{0,rr} + 1/r\theta_{0,r}) \quad (3.11) \quad \text{and to the}$$

first order are

$$w_{1,rr} + w_{1,r} - (D_2^{-1} + \frac{M^2}{r^2})w_1 = -G\theta_1 \quad (3.12)$$

$$\theta_{1,rr} + (1/r)\theta_{1,r} = -P(w_{0,rr}^2 + \lambda^2/r^4) \quad (3.13)$$

$$C_{1,rr} + (1 - \lambda Sc)(1/r)C_{1,r} = -(\frac{ScSo}{N})(\theta_{1,rr} + (1/r)\theta_{1,r}) \quad (3.14)$$

The corresponding boundary conditions are

$$w_0(1) = 0, w_0(s) = 0, \quad (3.15)$$

$$\theta_0(1) = 0, \theta_0(s) = m_1 \quad (3.16)$$

$$C_o(1) = 0, \quad C_o(s) = m_2$$

and

$$w_1(1) = 0, w_1(s) = 0, \quad (3.17)$$

$$\theta_1(1) = 0, \theta_1(s) = 0 \quad (3.18)$$

$$C_1(1) = 0, \quad C_1(s) = 0$$

The differential equations (3.9)-(3.14) have been discussed numerically by reducing the differential equations into difference equations which are solved using Gauss-Seidel Iteration method. The differential equations involving θ_0, θ_1 , and w_1 are reduced to the following difference equations

$$(1 - \frac{h}{2r_i})\theta_{0,i-1} - 2\theta_{0,i} + ((1 + \frac{h}{2r_i})\theta_{0,i+1} = -\alpha h^2 \quad (3.19)$$

$$\begin{aligned} (1 - \frac{h}{2r_i})C_{0,i-1} - 2C_{0,i} + ((1 + \frac{h}{2r_i})C_{0,i+1} = \\ -(\frac{ScS_0}{N})(1 - \frac{h}{2r_i})\theta_{0,i-1} - 2\theta_{0,i} + ((1 + \frac{h}{2r_i})\theta_{0,i+1} \end{aligned} \quad (3.20)$$

$$\begin{aligned} (1 - \frac{h(1-\lambda)}{2r_i})w_{0,i-1} - (2 + h^2(D_2^{-1} + (M^2 / r^2)))w_{0,i} + \\ + (1 + \frac{h(1-\lambda)}{2r_i})w_{0,i+1} = -Gh^2(\theta_{0,i} + NC_{0,i}) \end{aligned} \quad (3.21)$$

$$(1 - \frac{h}{2r_i})\theta_{1,i-1} - (2)\theta_{1,i} + ((1 + \frac{h}{2r_i})\theta_{1,i+1} = Ph(w_{0,i}^2). \quad (3.20)$$

$$\begin{aligned} (1 - \frac{h}{2r_i})C_{1,i-1} - 2C_{1,i} + ((1 + \frac{h}{2r_i})C_{1,i+1} = - \\ (\frac{ScS_0}{N})(1 - \frac{h}{2r_i})\theta_{1,i-1} - 2\theta_{1,i} + ((1 + \frac{h}{2r_i})\theta_{1,i+1}) \end{aligned} \quad (3.21)$$

$$\begin{aligned} (1 - \frac{h}{2r_i})w_{1,i-1} - (2 + h^2(D_2^{-1} + (M^2 / r^2)))w_{1,i} + (1 + \frac{h}{2r_i})w_{1,i+1} \\ = -Gh^2(\theta_{1,i} + NC_{1,i}) \end{aligned} \quad (3.22)$$

(I = 1, 2, 21)

where h is the step length taken to be 0.05 together with the following conditions

$$\theta_{0,0} = 1, \quad \theta_{0,17} = m_1$$

$$\theta_{1,0} = 0, \quad \theta_{1,17} = m_1$$

$$C_{0,0} = 1, \quad C_{0,17} = m_2$$

$$C_{1,0} = 0, \quad C_{1,17} = m_2$$

$$w_{0,0} = 0, \quad w_{0,17} = 0$$

$$w_{1,0} = 0, \quad w_{1,17} = 0$$

All the above difference equations are solved using Gauss-Seidel iterative method to the fourth decimal accuracy.

4. Case of temperature dependent heat source

In the presence of temperature dependent heat sources the equation of energy (3.2) takes the form

$$\begin{aligned} \rho C_p(uT_r) = k_1(T_{rr} + T_r / r) + \mu(2(u_r^2 + u^2 / r^2) + w_r^2) + \\ + (\mu / k + \sigma \mu_e^2 H_o^2)(u^2 + w^2) + Q(T_e - T) \end{aligned} \quad (4.1)$$

Making use of (2.6) in (4.1) the above energy equation reduces to

$$T_{rr} + (1 - au_a / \nu) T_r / r + \mu(2(u^2 / r^2) + w_r^2) + (\mu / k + \sigma \mu_e^2 H_o^2)(u^2 + w^2) + Q(T_e - T) \quad (4.2)$$

Making use of non-dimensional variables(3.8) the above equation reduces to

$$w_{rr} + (1/r) w_r - (D_2^{-1} + (M^2 / r^2)) w = -G \theta \quad (4.3)$$

$$\theta_{rr} + \theta_r / r - \alpha \theta = -PE_c (w_r^2 + \lambda^2 / r^4) \quad (4.4)$$

$$C_{rr} + C_r / r = -(\frac{S_c S_0}{N})(\theta_{rr} + \theta_r / r) \quad (4.5)$$

Substituting (3.7) in equations (4.3) - (4.5) and separating the like powers of Ec

the equations to the zeroth order are

$$w_{o,rr} + (1/r) w_{o,r} - (D_2^{-1} + \frac{M^2}{r^2}) w_o = -G \theta_o \quad (4.6)$$

$$\theta_{o,rr} + (1/r) \theta_{o,r} - \alpha \theta_o = 0 \quad (4.7)$$

$$C_{o,rr} + C_{o,r} / r = -(\frac{S_c S_0}{N})(\theta_{o,rr} + \theta_{o,r} / r) \quad (4.8)$$

and to the first order are

$$w_{1,rr} + (1/r) w_{1,r} - (D_2^{-1} + \frac{M^2}{r^2}) w_1 = -G \theta_1 \quad (4.9)$$

$$\theta_{1,rr} + (1/r) \theta_{1,r} - \alpha \theta_1 = -P(w_{o,r}^2 + \lambda^2 / r^4) \quad (4.10)$$

$$C_{1,rr} + C_{1,r} / r = -(\frac{S_c S_0}{N})(\theta_{1,rr} + \theta_{1,r} / r) \quad (4.11)$$

The corresponding boundary conditions are

$$w_1(1) = 0, w_1(s) = 0, \quad (4.12)$$

$$\theta_1(1) = 0, \theta_1(s) = 0 \quad (4.13)$$

$$C_1(1) = 0, C_1(s) = 0 \quad (4.14)$$

The differential equations (4.5)-(4.11) have been discussed numerically by reducing the differential equations into difference equations which are solved using Gauss-Seidel Iteration method. The differential equations involving θ_1 , and w_1 are reduced to the following difference equations

$$(1 - \frac{h}{2r_i}) \theta_{0,i-1} - (2 + \alpha h^2) \theta_{0,i} + ((1 + \frac{h}{2r_i}) \theta_{0,i+1} = -\alpha h^2 \quad (4.15)$$

$$\begin{aligned} (1 - \frac{h}{2r_i})C_{0,i-1} - 2C_{0,i} + ((1 + \frac{h}{2r_i})C_{0,i+1} = - \\ (\frac{S_c S_0}{N}) ((1 - \frac{h}{2r_i})\theta_{0,i-1} - 2\theta_{0,i} + ((1 + \frac{h}{2r_i})\theta_{0,i+1}) \end{aligned} \quad (4.16)$$

$$\begin{aligned} (1 - \frac{h}{2r_i})w_{0,i-1} - (2 + h^2(D_2^{-1} + (M^2 / r^2)))w_{0,i} + (1 + \frac{h}{2r_i})w_{0,i+1} \\ = -Gh^2(\theta_{0,i} + NC_{0,i}) \end{aligned} \quad (4.17)$$

$$(1 - \frac{h}{2r_i}) \theta_{1,i-1} - (2 + \alpha h^2)\theta_{1,i} + ((1 + \frac{h}{2r_i}) \theta_{1,i+1} = Ph(\lambda^2 / r^4 + w_{0,i}^2). \quad (4.18)$$

$$\begin{aligned} (1 - \frac{h}{2r_i}) C_{1,i-1} - 2C_{1,i} + ((1 + \frac{h}{2r_i})C_{1,i+1} = - (\frac{S_c S_0}{N})(1 - \frac{h}{2r_i}) \theta_{1,i-1} - \\ - 2\theta_{1,i} + ((1 + \frac{h}{2r_i})\theta_{1,i+1} \end{aligned} \quad (4.19)$$

$$\begin{aligned} (1 - \frac{h}{2r_i})w_{1,i-1} - (2 + h^2(D_2^{-1} + (M^2 / r^2)))w_{1,i} + (1 + \frac{h}{2r_i})w_{1,i+1} \\ = -Gh^2(\theta_{1,i} + NC_{1,i}) \end{aligned} \quad (4.20)$$

(I = 1, 2,21)

Where h is the step length taken to be 0.05 together with the following conditions

$$\theta_{0,0} = 1, \quad \theta_{0,17} = m_1$$

$$\theta_{1,0} = 0, \quad \theta_{1,17} = m_1$$

$$C_{0,0} = 1, \quad C_{0,17} = m_2$$

$$C_{1,0} = 0, \quad C_{1,17} = m_2$$

$$w_{0,0} = 0, \quad w_{0,17} = 0$$

$$w_{1,0} = 0, \quad w_{1,17} = 0$$

All the above difference equations are solved using Gauss-Seidel iterative method to the fourth decimal accuracy.

The shear stress on the pipe is given by

$$\tau' = \mu \left(\frac{\partial w}{\partial r} \right)_{r=a,b}$$

which in the non-dimensional reduces to

$$\tau = \tau' / (\mu^2 / a^2) = (w_r)_{r=1,s} = (w_{0,r} + E_\epsilon w_{1,r})_{r=1,s}$$

The heat transfer through the pipe to the flow per unit area of the pipe surface is given by

$$q = k_1 \left(\frac{\partial T}{\partial r} \right)_{r=a,b}$$

which in the non-dimensional form is

$$Nu = \left(\frac{qa}{k_1(T_1 - T_e)} \right) = \left(\frac{\partial \theta}{\partial r} \right)_{r=1,s}$$

The mass transfer through the pipe to the flow per unit area of the pipe surface is given by

$$q_1 = D_1 \left(\frac{\partial C}{\partial r} \right)_{r=a,b}$$

which in the non-dimensional form is

$$Sh = \left(\frac{q_1 a}{D_1(C_1 - C_e)} \right) = \left(\frac{\partial C}{\partial r} \right)_{r=1,s}$$

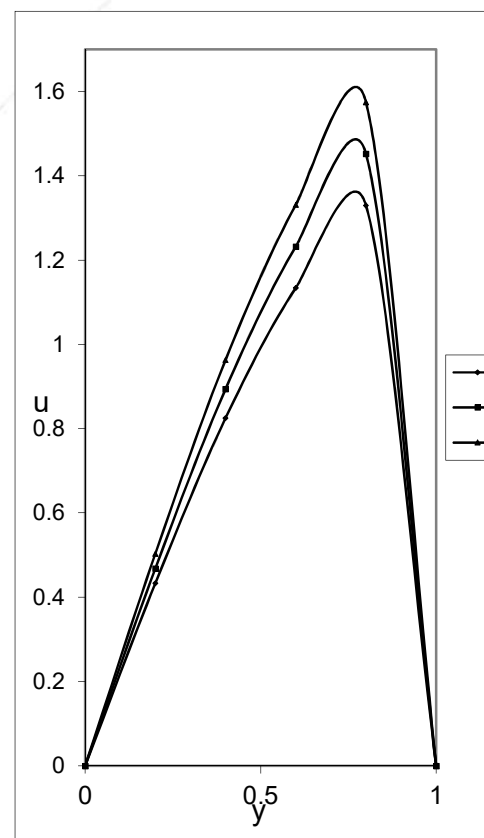
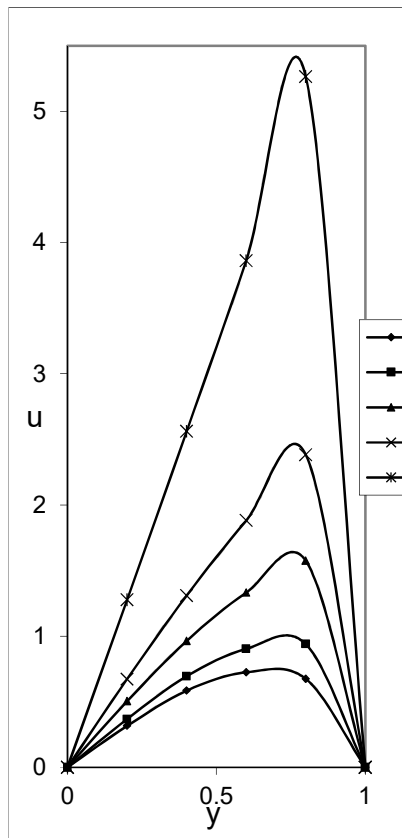
5. Discussion of the results

The convection flow sets in the presence of the heat source which is assumed to be constant (CS) or dependent on the temperature (TDS) in the fluid region. The analysis has been carried out when the outer cylinder is at a higher temperature than that of the inner cylinder $m_1=2$. The actual flow is along the gravitational field and hence the axial velocity (w) in the vertical direction represents the actual flow. $W>0$ indicates the reversal flow. For computational purposes we have chosen the non-dimensional temperature (θ) on the outer cylinder to be $m_1=2$, on the inner cylinder it continues to be 1. The velocity, the temperature and the concentration are exhibited in figs.1-21 in constant source case and in figs.22-41 in temperature dependent source case. We find from fig1&22 that no reversal appears in the region for $G>0$ and reversal flow appears for $G<0$ in both CS and TDS cases. Also we find that the magnitude of W in CS case at any point is greater than that at the corresponding point in the TDS case. Figs.2,3,23&24 correspond to the behavior of W for variations in D^{-1} and M . We find that in both cases lesser the permeability of the porous medium smaller the magnitude of W at any point in the fluid region (figs.2&23). Also $|W|$ retards with increase in the Hartmann number M (figs.3&24). Figs.4&25 show the variation of W with the buoyancy ratio N . It is observed that when the molecular buoyancy force dominates over the thermal buoyancy force $|W|$ enhances with N when the two forces act in the same direction and for the forces acting in opposite directions $|W|$ decreases with $|N|$ in both CS and TDS cases with maximum attained at midhalf of the region. Also lesser the permeability of the porous medium greater the magnitude of W in both the cases (figs.5&26). The influence of the Soret effect on the velocity distribution is exhibited in figs.6&27. We find that when So increases through positive/negative values, $|W|$ enhances in both CS and TDS cases. We notice a reversal flow in the annular region for $So=-1$. The presence of heat sources (CS & TDS) on W can be noticed from figs.7&28. No such reversal flow appears both in the CS and TDS cases. With increase in the strength of the heat source we find an enhancement in $|W|$, while $|W|$ decreases in the case of a heat sink (fig.7). Also $|W|$ decays with increase in the strength of the heat generating source (fig.28). $|W|$ in the CS case is much greater than that in the heat generation source at the corresponding points.

The figs.8-14 and 28-35 represent the temperature distribution (θ) for different variations of G, R, Sc, S_0, N, D^{-1} and α in CS and TDS cases respectively. In presence of convection current the temperature gradually increases from its given value on the inner cylinder to attain the higher prescribed value on the cylinder for all G . We find that in a given porous medium the temperature increases marginally with increase in G (fig.8&29). We find that for all variations in the parameters the temperature in the constant heat source is much greater than that in the TDS case at all corresponding points in the flow region. The temperature for different values of D^{-1} and M are plotted in figs.9,10,31&32. We find that the temperature increases with increase in D^{-1} . Thus lesser the permeability of the porous medium larger the temperature in the fluid region. Also the temperature experiences a depreciation with increase in M . Figs.11&32 show the variation of temperature with increase in the buoyancy ratio N . We notice that when the molecular buoyancy force dominates over the thermal buoyancy force the temperature in the CS case decreases with N irrespective of the directions of the buoyancy forces, while in the case of TDS it enhances with N when the buoyancy forces act in the same direction and decrease with $|N|$ when they act in opposite directions. Also we find from figs.12&33 that lesser the molecular diffusivity larger the temperature in the entire fluid region in both CS and TDS cases. The influence of the Soret effect on θ can be seen from figs.13&34. In both CS and TDS cases we find that the temperature enhances with increase in Soret parameter $|S_0| (<0)$. Thus the inclusion of the Soret effect on temperature is to enhance it in the

entire fluid region. From fig. 14 it is noticed that the temperature enhances with increase in the strength of the heat source while it decays with increase in the strength of the heat sink. In the case of TDS we notice that the temperature decreases in the flow region with increase in the strength of the heat generating source. The temperature at any point in the fluid region in the CS case is larger than that in the TDS case at the corresponding points with maximum attained on the outer cylinder.

Figs. 15-21 and 36-41 represent the concentration distribution (C) for different variations of G, D, Sc, S_0, N and α . The concentration for all variations is observed to be positive. This indicates that the actual concentration is greater than the equilibrium concentration. We find that the concentration in the CS case is smaller than that in the TDS case. The concentration gradually rises from its prescribed value on the inner cylinder, reaches its maximum at $r=1.5$ and then falls to attain the prescribed value on the outer cylinder $r=2$. Figs. 15 & 36 show that the concentration increases with increase in G in both CS and TDS cases with maximum attained at $r=1.5$. The variation of C with D^{-1} and M can be seen from figs. 16, 17, 37 & 38. It is found that the concentration experiences a depreciation with lowering of the permeability of the porous medium in both CS and TDS cases. An increase in the strength of the magnetic field enhances in the flow region. The variation of C with buoyancy ratio N shows that when the molecular buoyancy force dominates over the thermal buoyancy force the concentration decays irrespective of the directions of the buoyancy forces. In the case of CS maximum value of C occurs at $r=1.5$ while in the TDS case it occurs at $r=1.6$. Also figs. 19 & 40 show that lesser the molecular diffusivity larger the concentration in the entire fluid region. An increase in $|S_0|$ (<0) enhances C in the flow region (figs. 20 & 41). The variation of C with α indicates that C enhances with increase in the strength of the heat source ($\alpha > 0$) and decreases with increase in $|\alpha| \leq 4$ and for further increase in $|\alpha| \geq 6$ we find that the concentration decreases in the region abutting the inner cylinder and enhances in the region adjacent to the outer cylinder (fig. 21). In the TDS case we find that the concentration depreciates with an increase in the strength of the heat generating source at all point in the flow region (fig. 42).



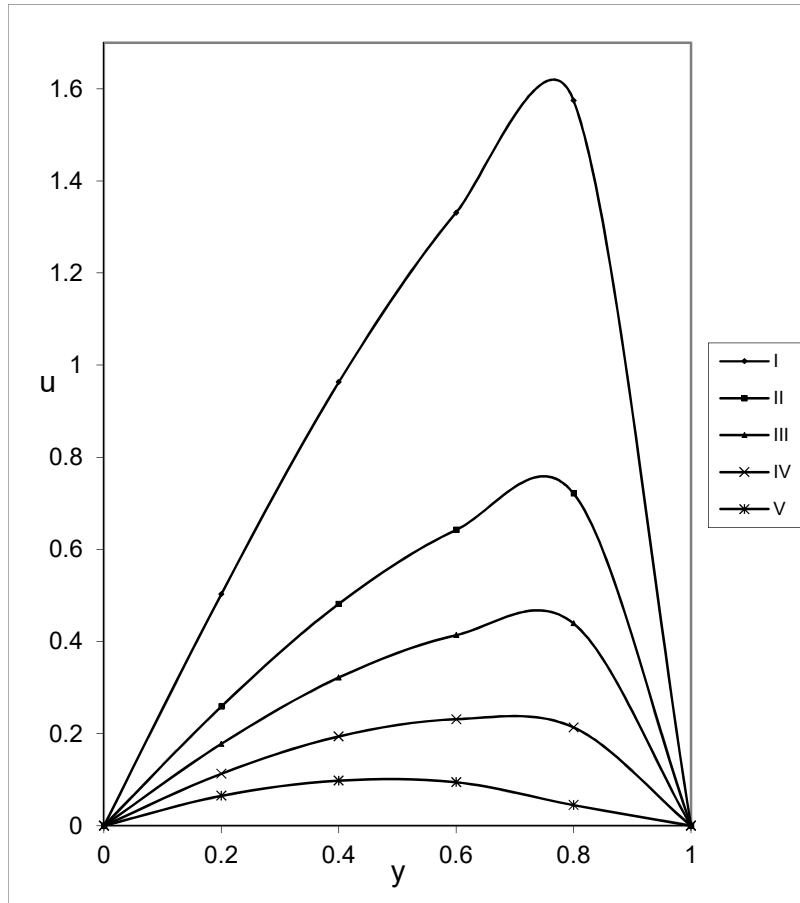


Fig.3 u with R
 $D^{-1}=3 \times 10^3$, $G=3 \times 10^3$, $Sc=1.3$

	I	II	III	IV
R	10^2	2×10^2	3×10^2	5×10^2

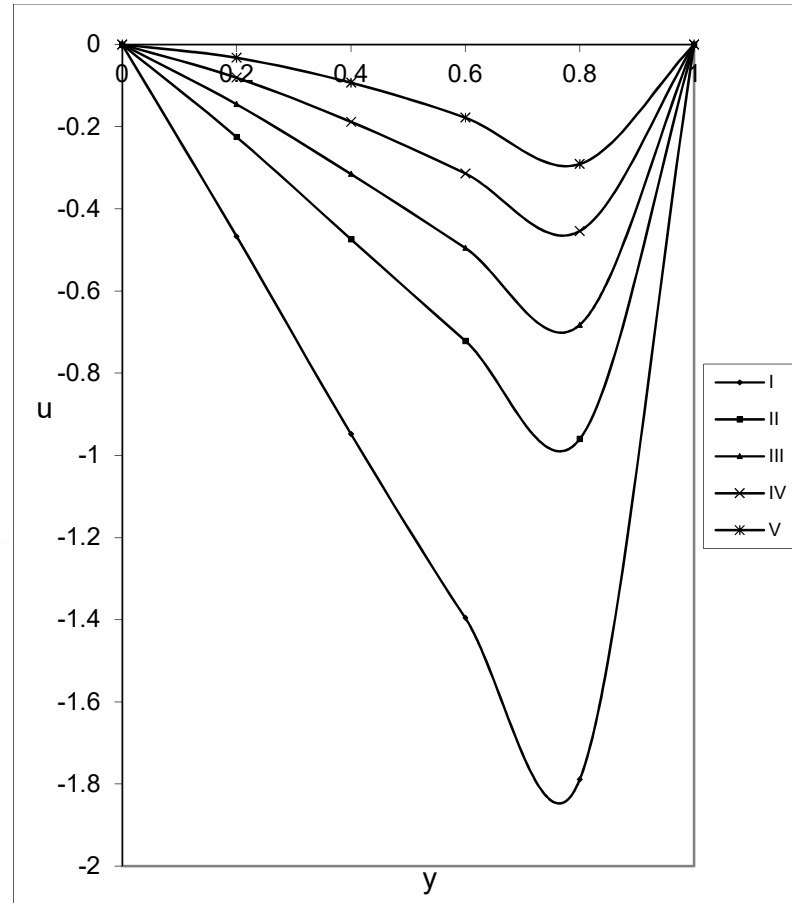


Fig.4 u with R

	I	II	III	IV
R	-10^2	-2×10^2	-3×10^2	-5×10^2

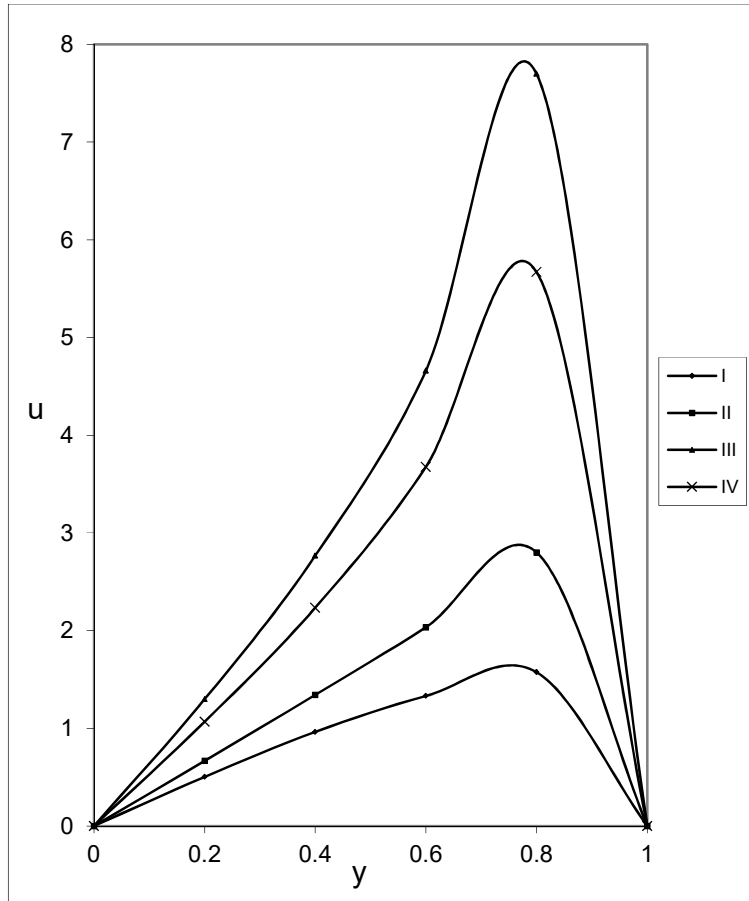


Fig.5 u with S_0
 $G=3 \times 10^3, D^{-1}=3 \times 10^3, Sc=1.3$

	I	II	III	IV
S_0	0.5	1.0	-0.5	-1.0

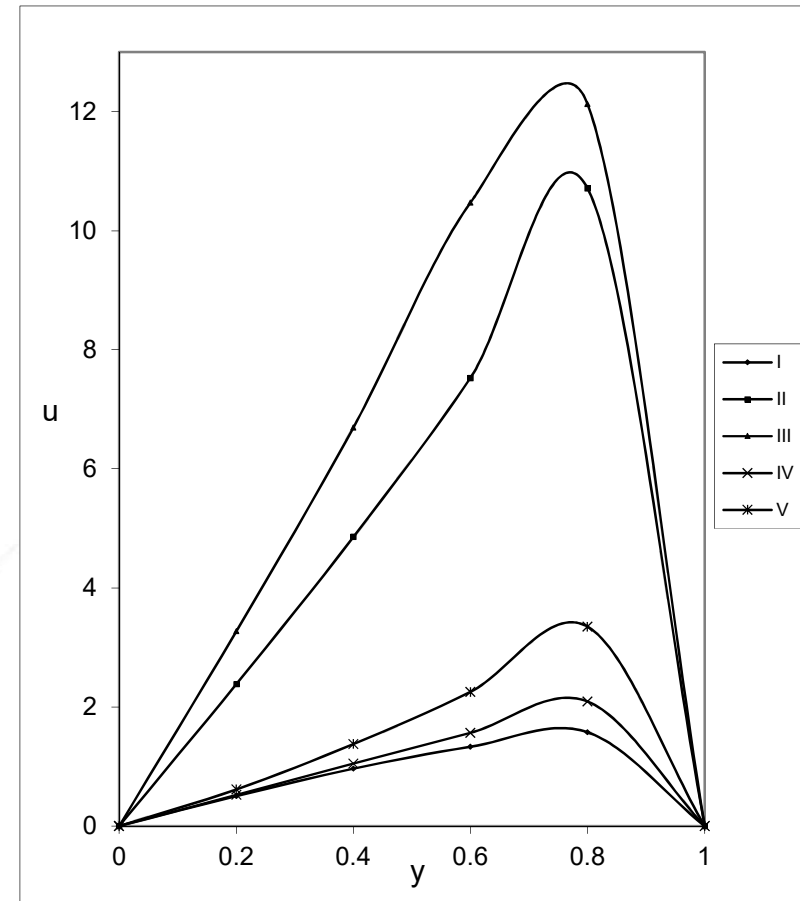


Fig.6 u with M
 $Sc=1.3, S_0=0.5, N=1$

	I	II	III
M	2	4	6

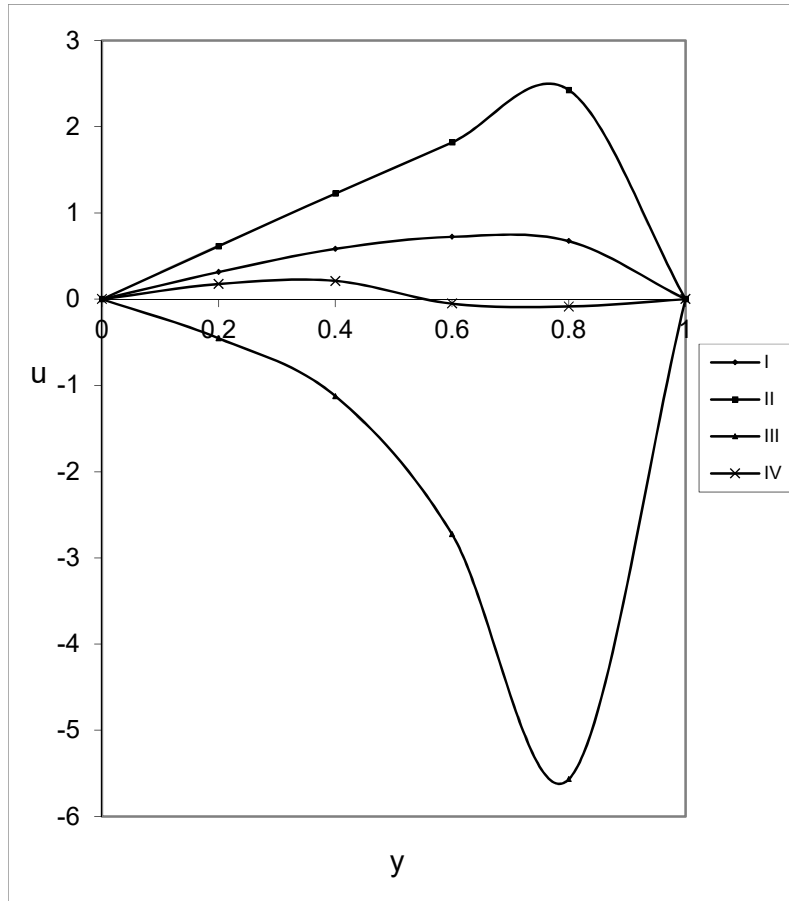


Fig.7 u with Sc
 $S_0=0.5, R=2 \times 10^2, G=3 \times 10^3$

	I	II	III	IV
S_0	1.3	2.01	0.24	0.6

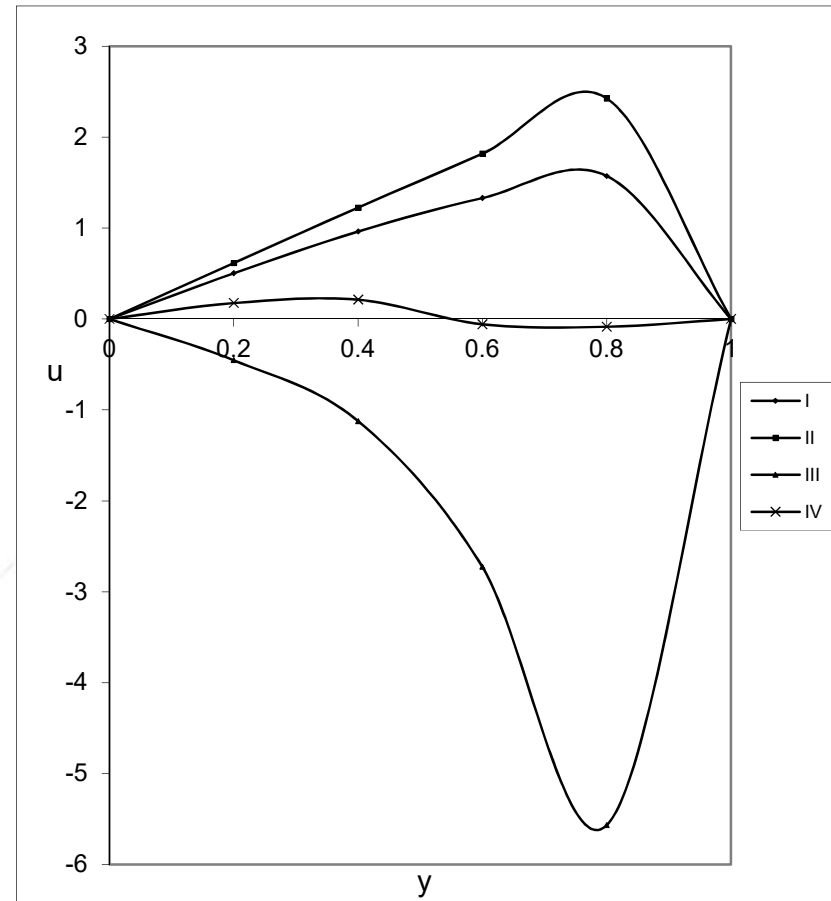


Fig.8 u with Ec
 $Sc=1.3, S_0=0.5, M=2$

	I	II	III	IV
Ec	0	0.1	0.3	0.7

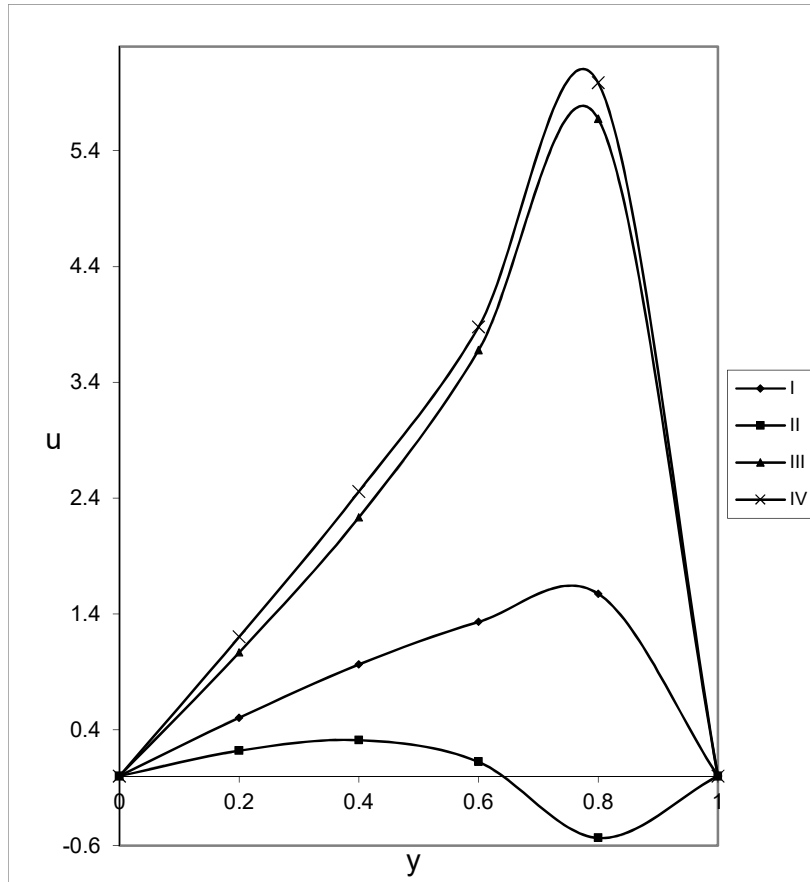


Fig.9 u with N
 $Sc=1.3, S_0=0.5, R=2 \times 10^2$

	I	II	III	IV
N	1	2	-0.5	-0.8

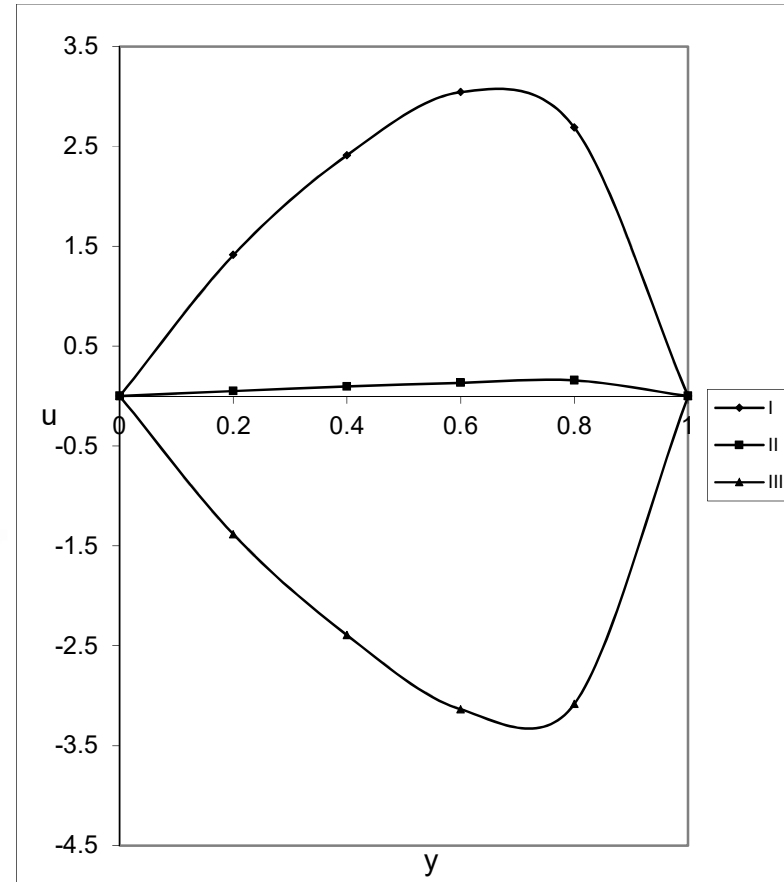


Fig.10 u with y
 $Sc=1.3, S_0=0.5, Ec=0.5$

	I	II	III
y	0.25	0.5	0.75

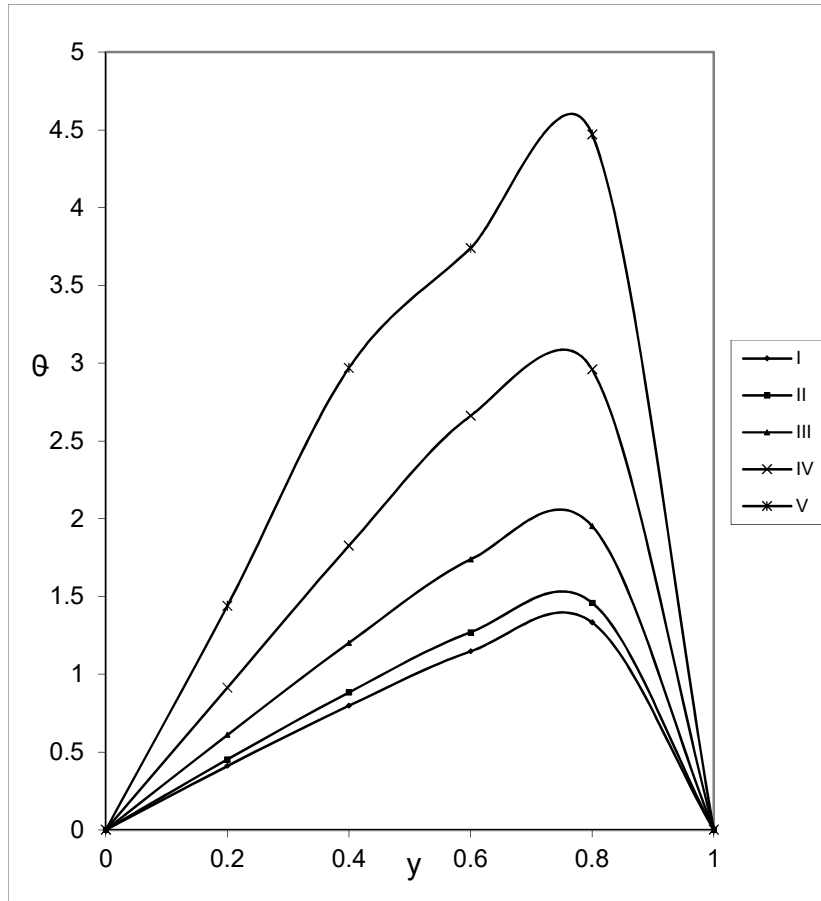


Fig.11 Variation of temperature(θ) with D^{-1}

$$G=3 \times 10^3, Sc=1.3, N=1$$

I	II	III	IV	V
$D^{-1} \ 10^3$	2×10^3	3×10^3	5×10^3	10^4

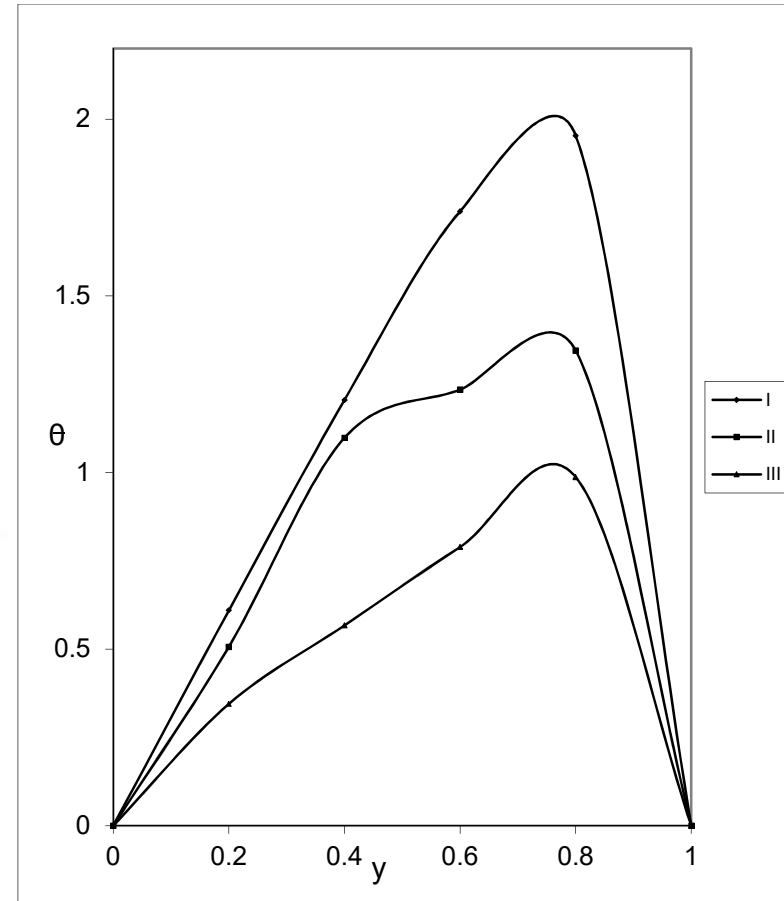


Fig.12 θ with Sc

$$D^{-1} = 3 \times 10^3, Sc=1.3, N=1$$

I	II	III
$G \ 10^3$	2×10^3	3×10^3

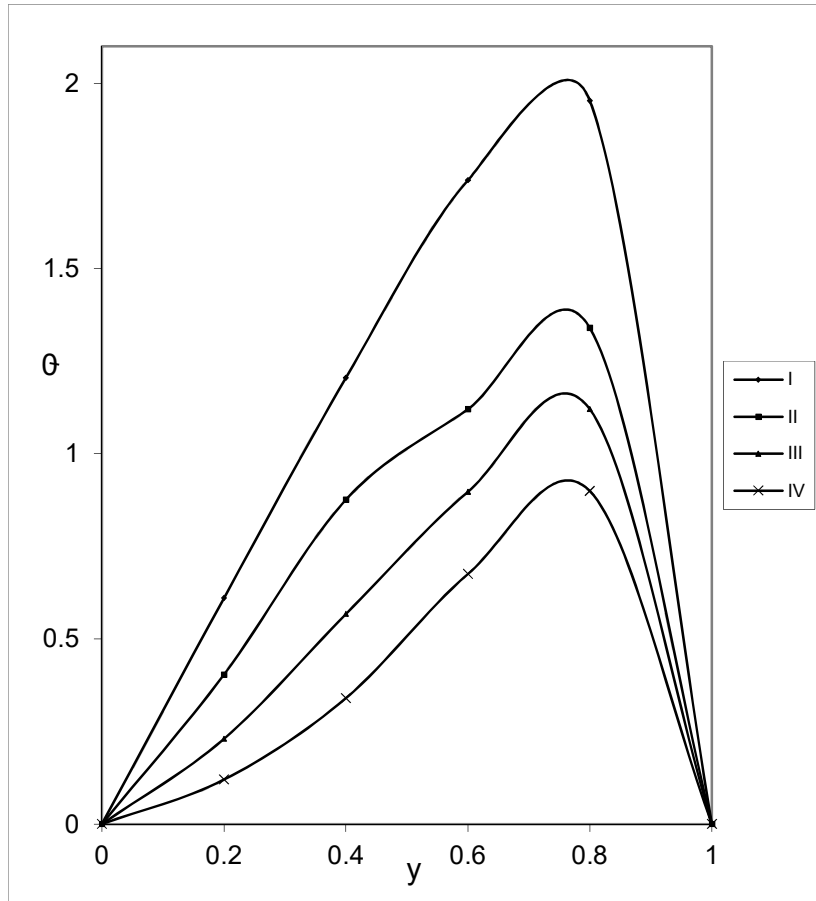


Fig.13 θ with R
 $D^{-1}=3 \times 10^3, G=3 \times 10^3, Sc=1.3$

	I	II	III	IV
R	10^2	2×10^2	3×10^2	5×10^2

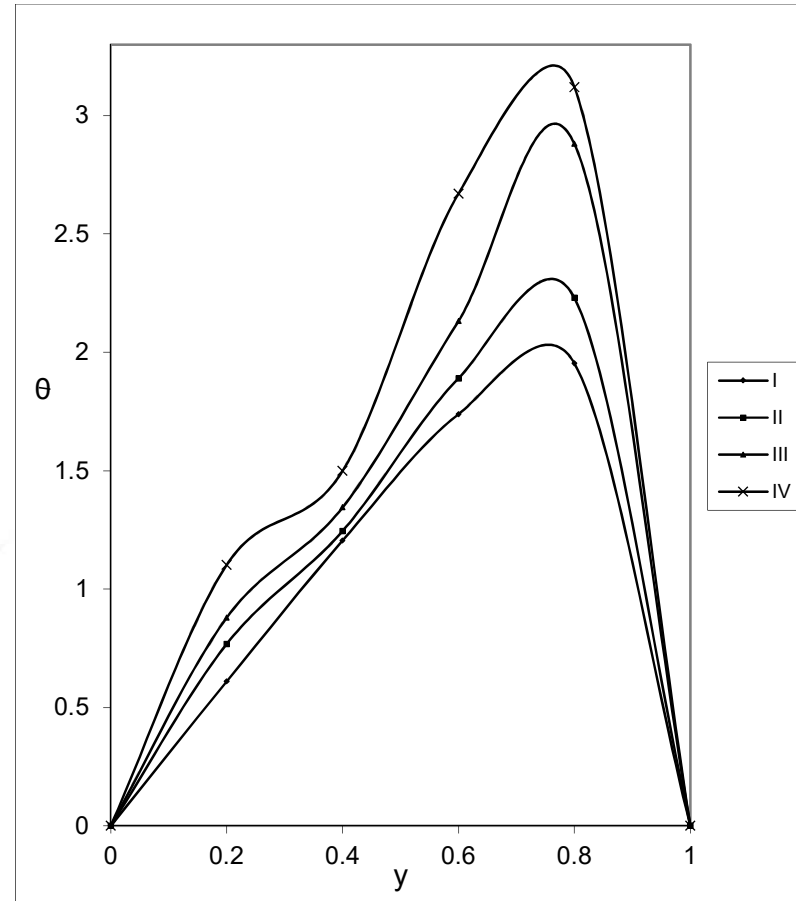
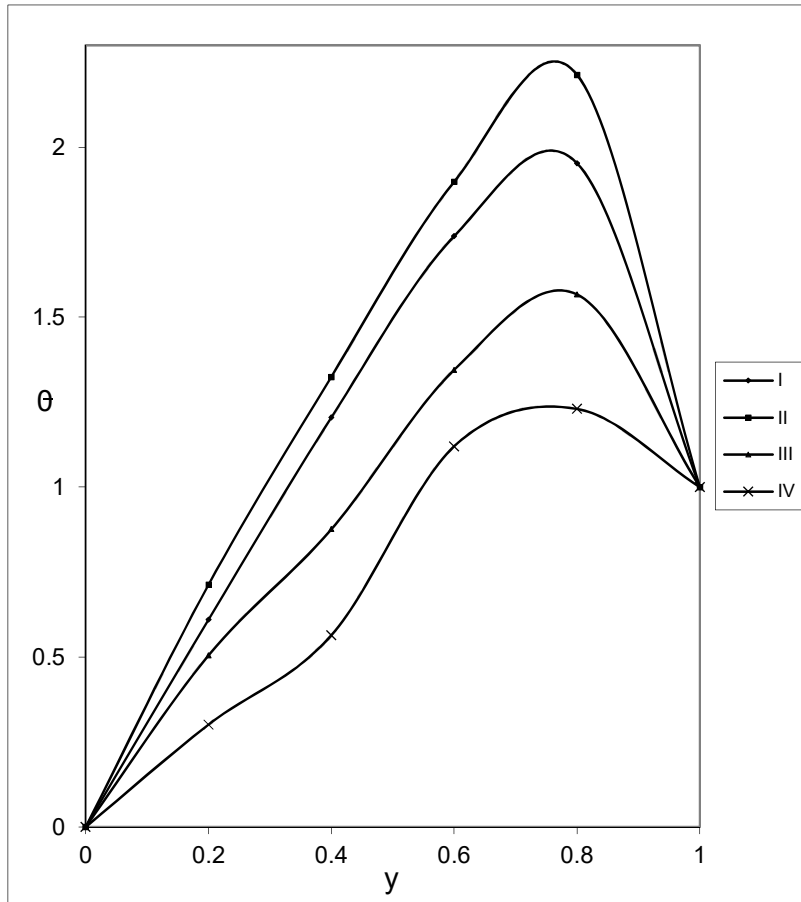
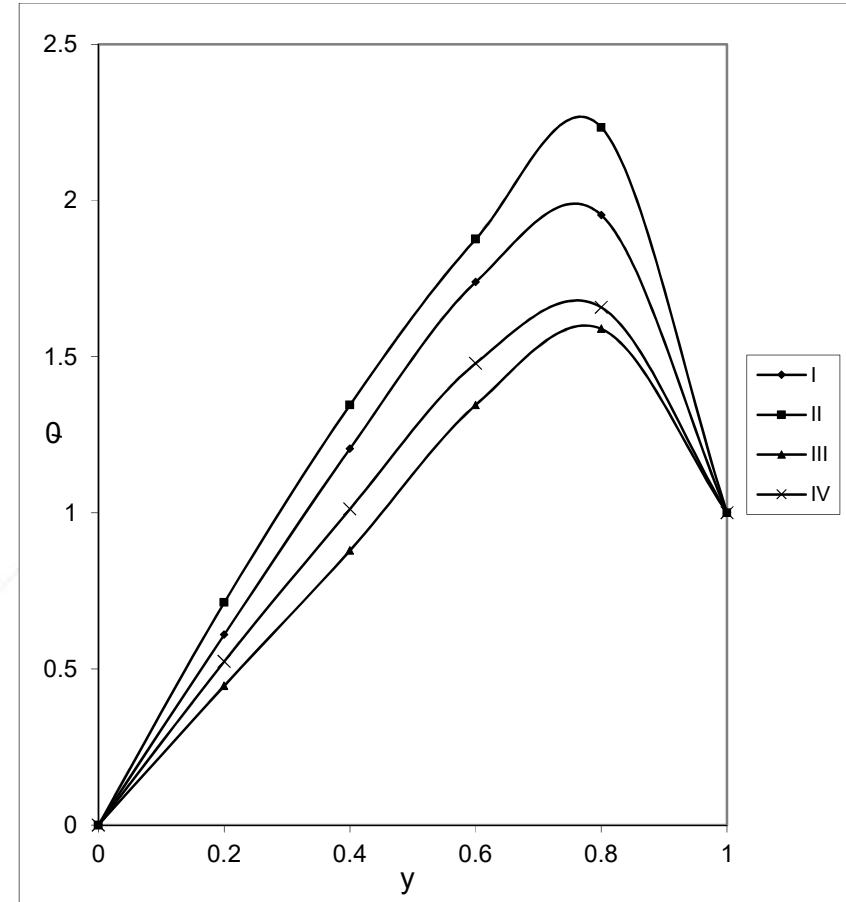


Fig.14 θ with R

	I	II	III	IV
R	-10^2	-2×10^3	-3×10^3	-5×10^2


Fig.16 θ with S_0
 $Sc=1.3, N=1, Ec=0.5$

	I	II	III	IV
S_0	0.5	1.0	-0.5	-1.0


Fig.17 θ with α
 $Sc=1.3, S_0=0.5, Ec=0.5, N=1$

	I	II	III
α	2	4	6

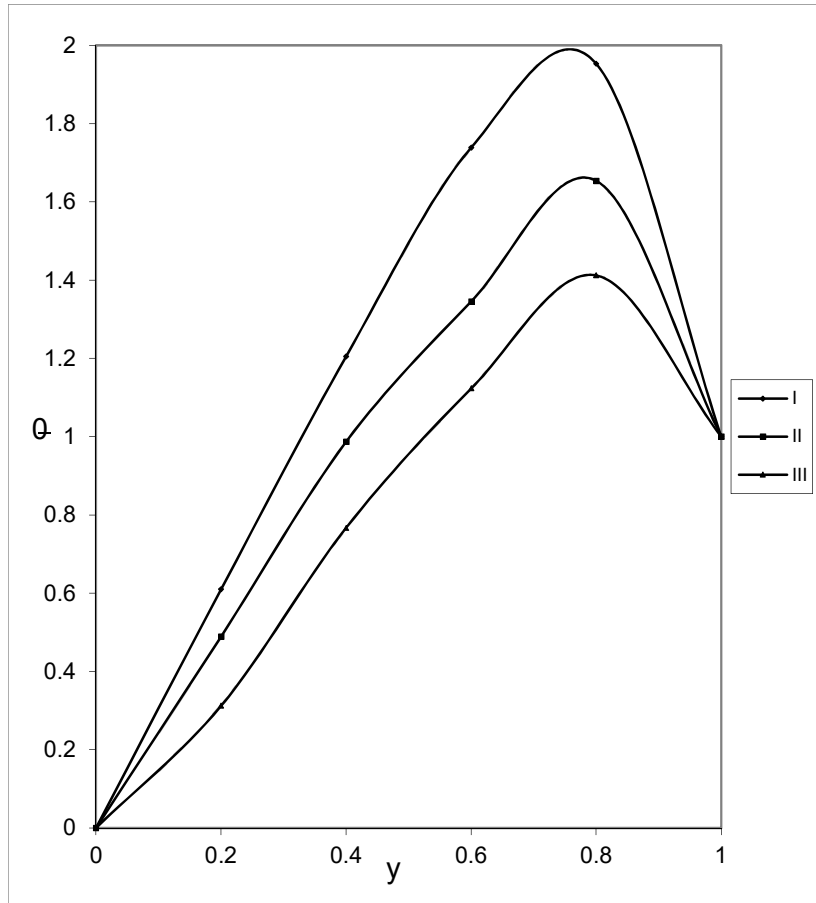


Fig.18 θ with α
 $Sc=1.3, S_0=0.5, Ec=0.5, N=1$

	I	II	III
α	2	4	6

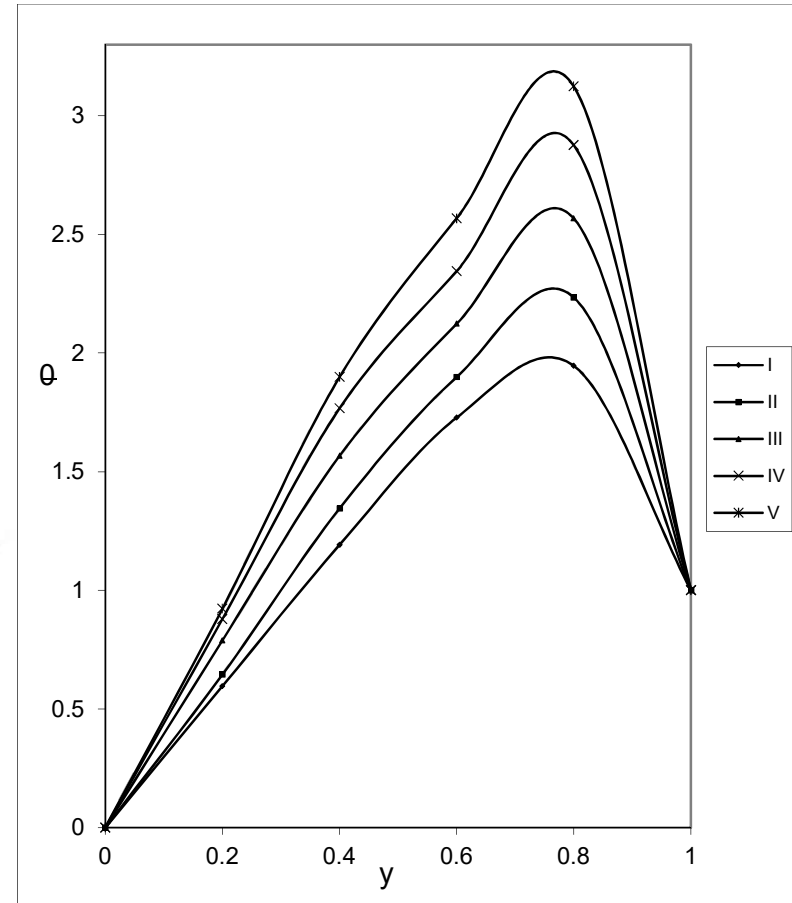
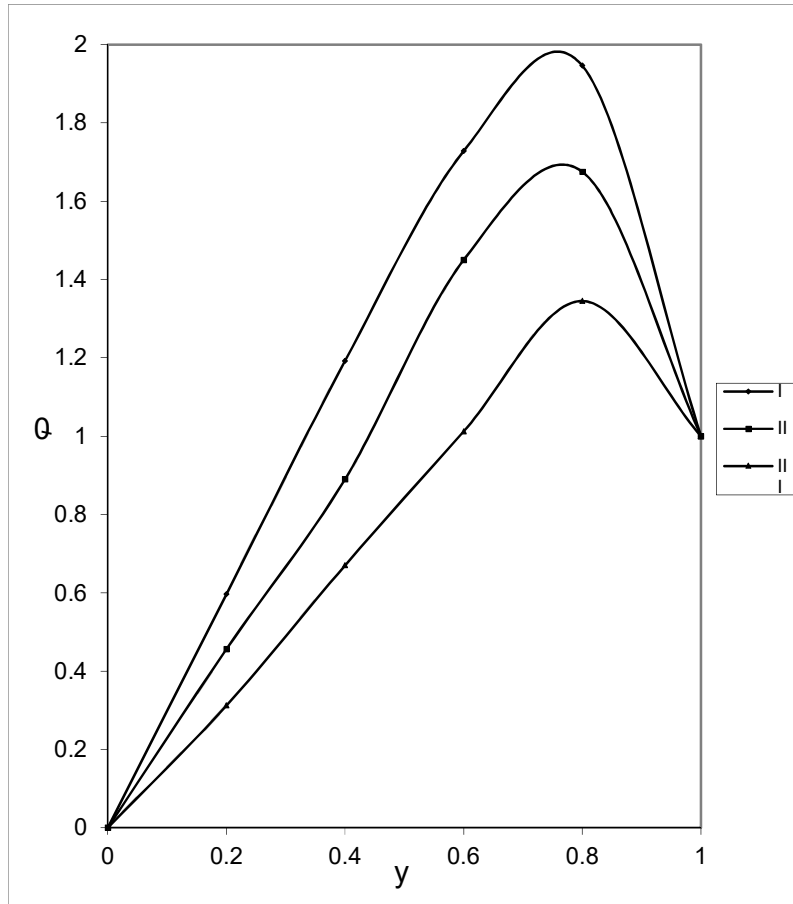
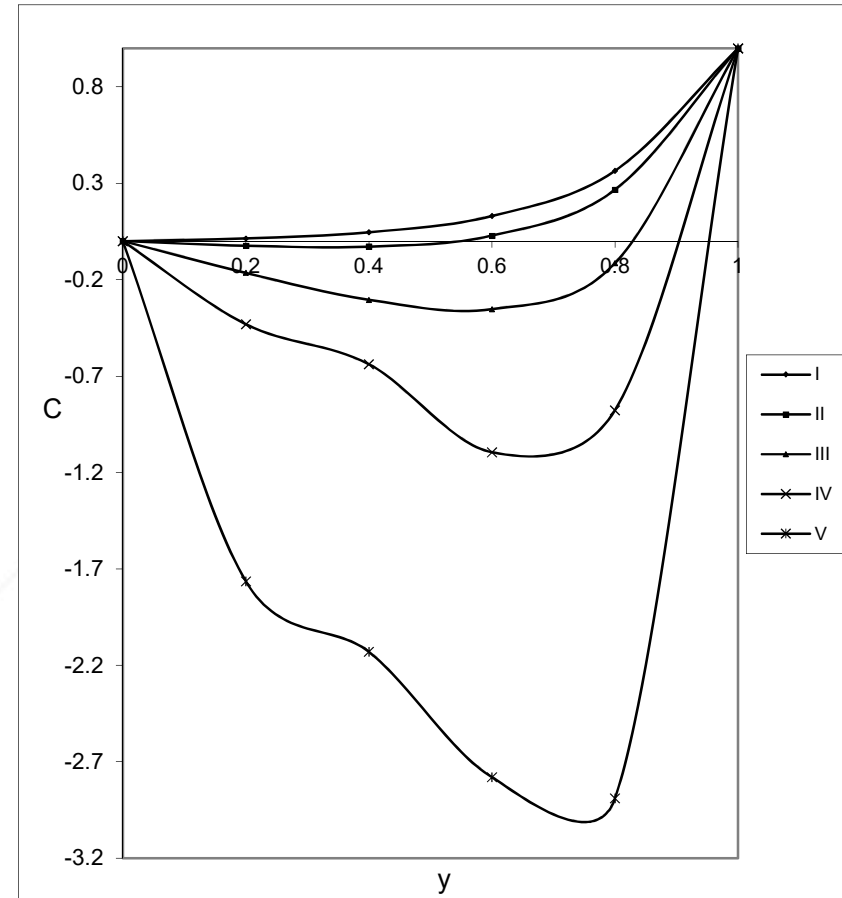


Fig.19 θ with α

	I	II	III	IV	V
Ec	0	0.1	0.3	0.5	0.7


Fig.20 θ with y
 $Sc=1.3, Sc=0.5, N=1, Ec=0.5$

I II III

 y 0.25 0.5 0.75

Fig.21 Variation of Concentration(c) with D^{-1}
 $G=3 \times 10^3, R=2 \times 10^2, Sc=1.3, N=1$

I II III IV V

 D^{-1} 10^3 2×10^3 3×10^3 5×10^3 10^4

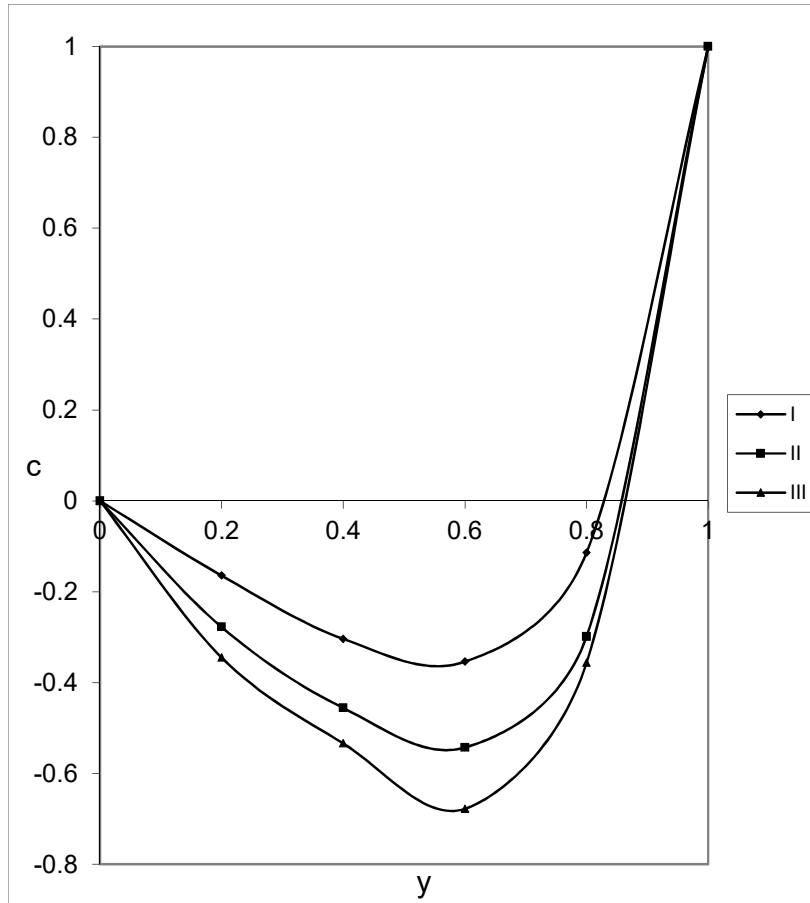
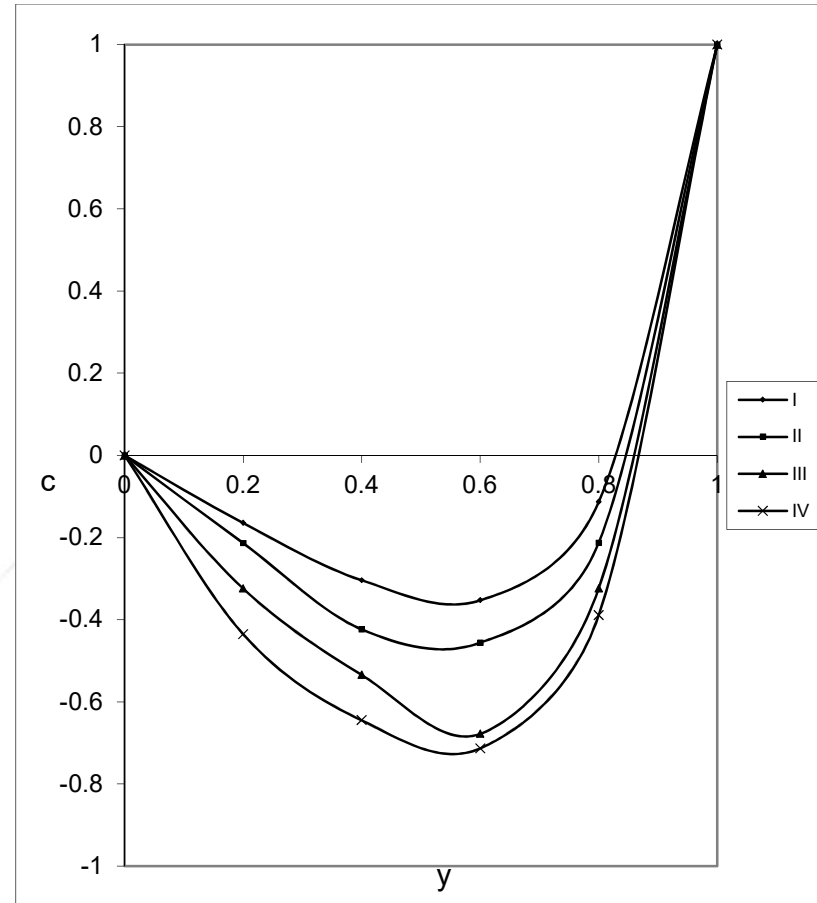


Fig.22 C with G

 $D^{-1}=2 \times 10^3, R=2 \times 10^2, N=1$

	I	II	III
G	10^3	2×10^3	3×10^3


Fig.23 c with α

	I	II	III	IV
R	10^2	2×10^2	3×10^2	5×10^2

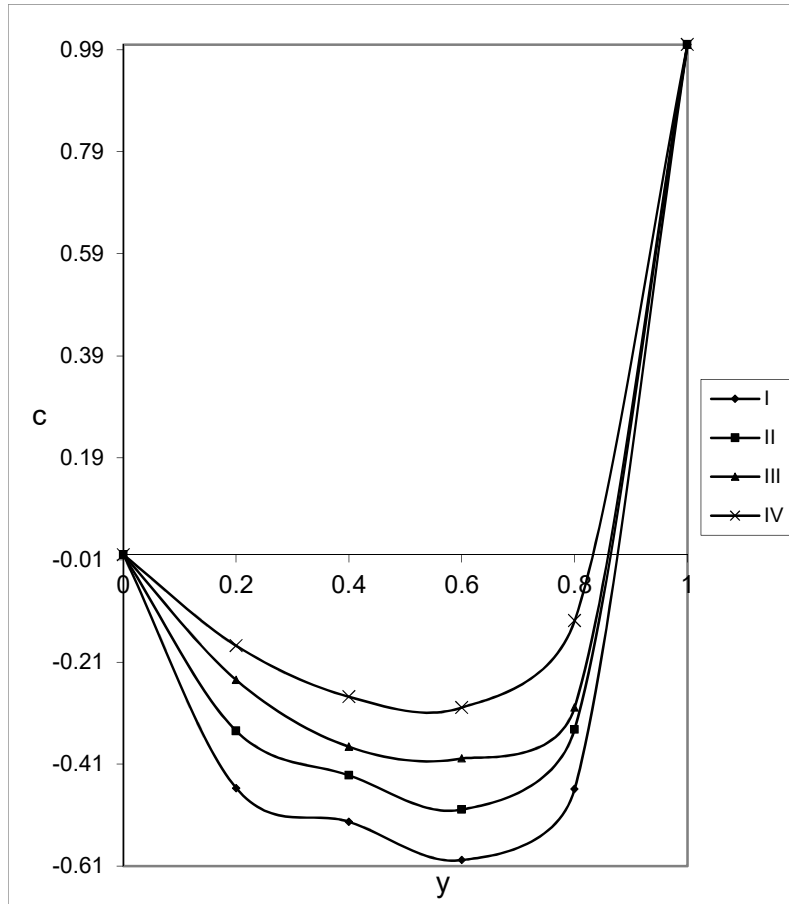


Fig.24 C with R

	I	II	III	IV
R	-10^2	-2×10^2	-3×10^2	-5×10^2

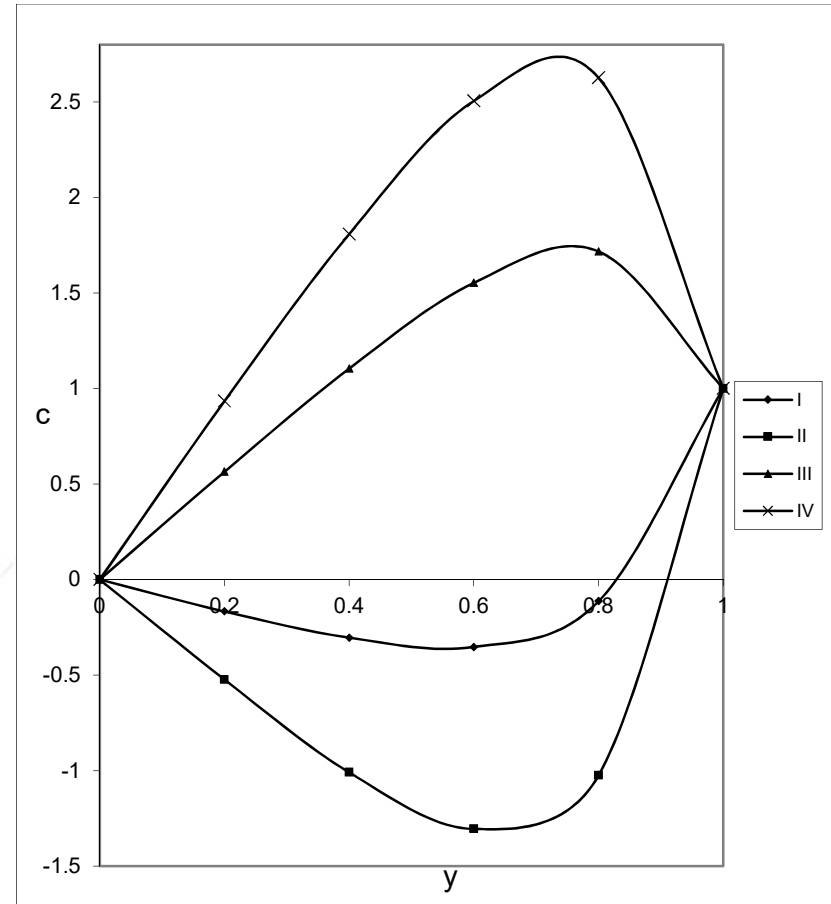


Fig.25 C with S_0

	I	II	III	IV
S_0	0.5	1.0	-0.5	-1.0

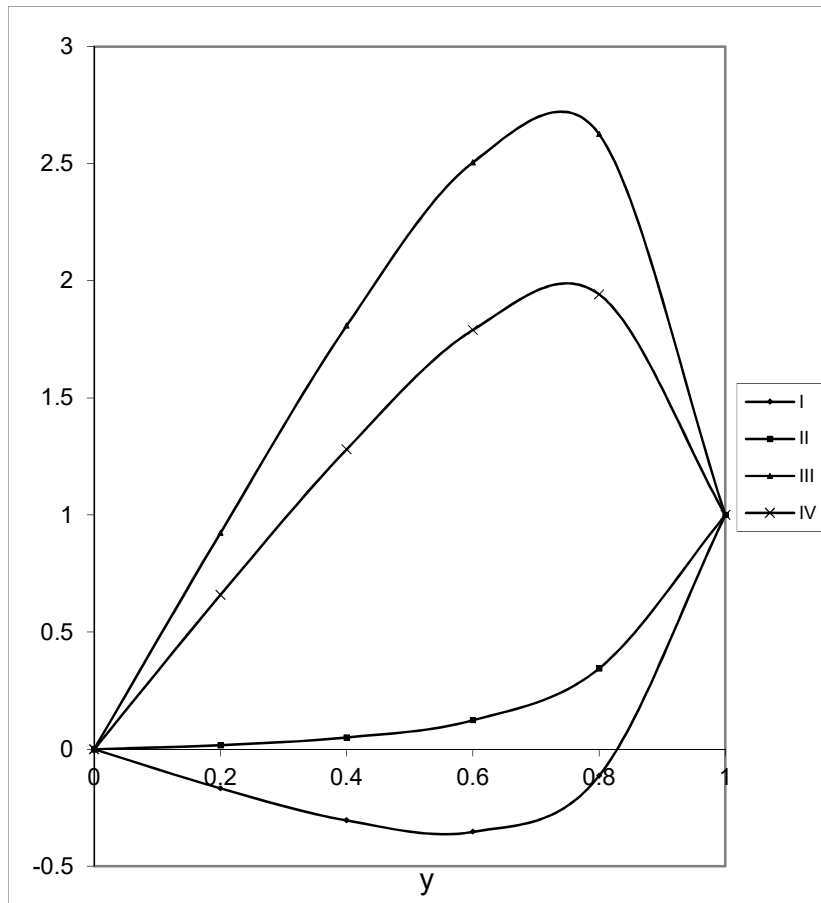


Fig.26 C with N
 $Sc=1.3, S_0=0.5, Ec=0.5$

	I	II	III	IV
N	1	2	-0.5	-0.8

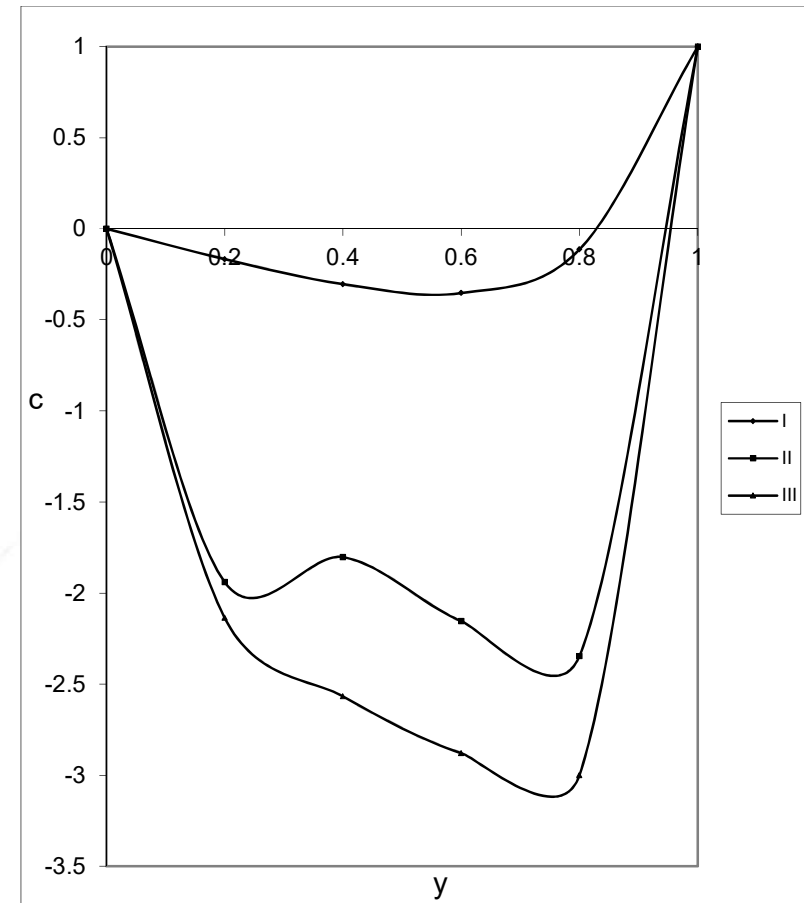


Fig.27 C with M
 $Sc = 1.3, S_0 = 0.5, N=1$

	I	II	III
M	2	4	6

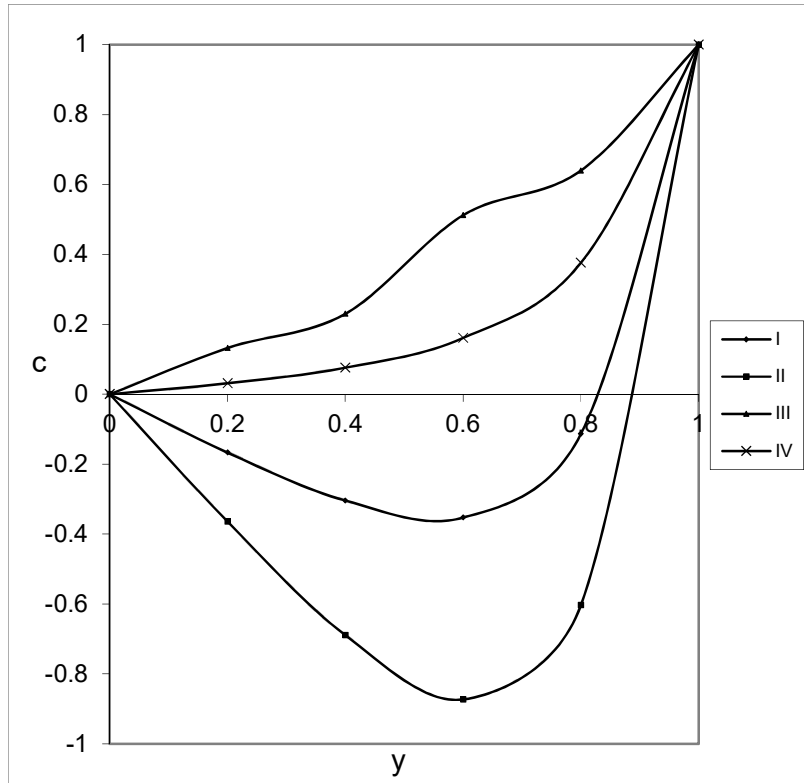


Fig.28 C with Sc
 $N=1, S_0=0.5, Ec=0.5, R=2 \times 10^2$

	I	II	III	IV
Sc	1.3	2.01	0.24	0.6

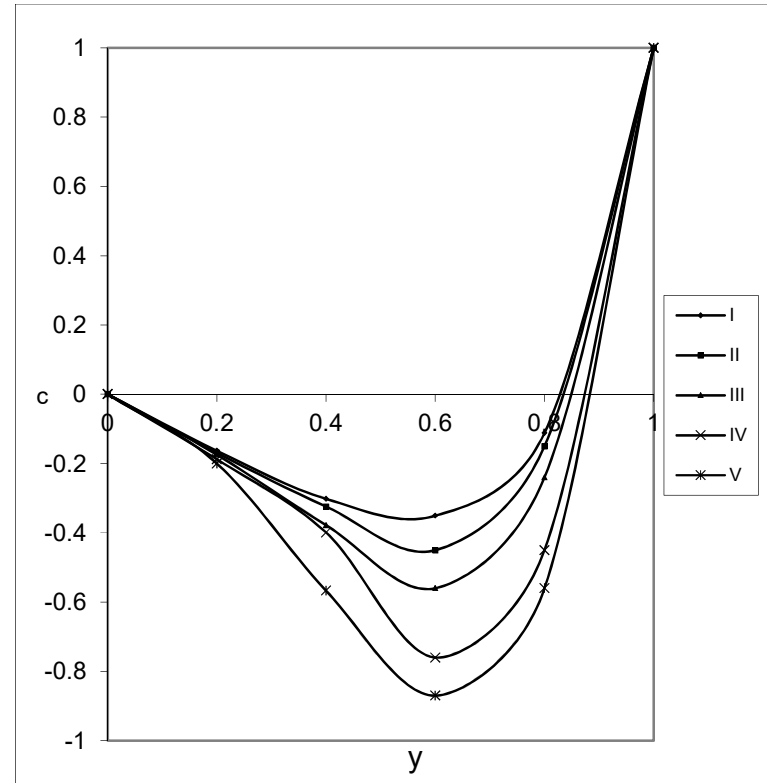


Fig.29 C with Ec
 $Sc=1.3, S_0=0.5, N=1, M=2$

	I	II	III	IV	V
Ec	0	0.1	0.3	0.5	0.7

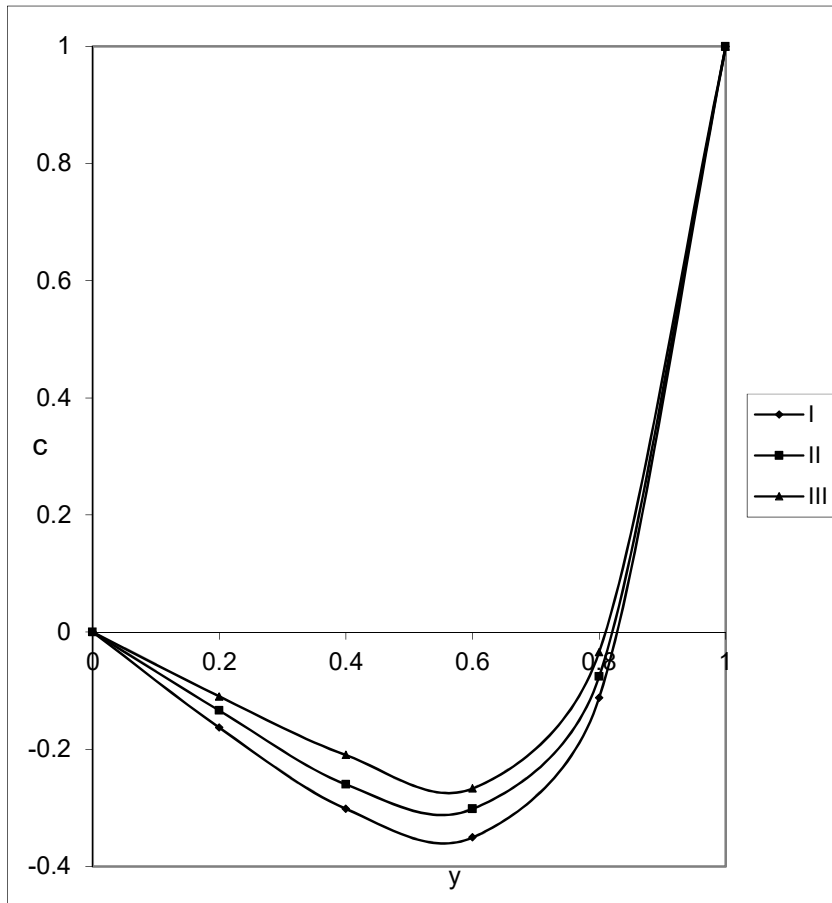


Fig.30 C with y
 $N=1, Sc=1.3, S_0=0.5, Ec=0.5$

	I	II	III
Y	0.25	0.5	0.75

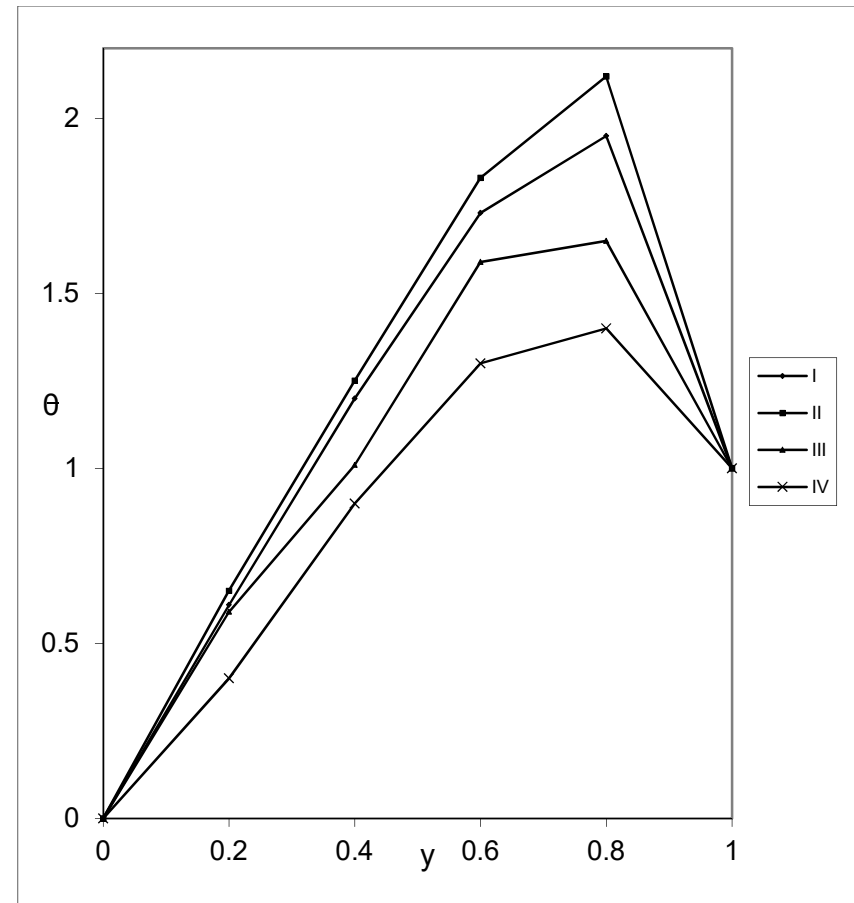


Fig.15 θ with S
 $Sc=1.3, N=1, Ec=0.5$

	I	II	III	IV
Sc	0.5	1.0	-0.5	-1.0

The rate of heat transfer on both the cylinders has been depicted in tables for different variations. We find that the rate of heat transfer on the heat transfer is positive and that on the outer cylinder it is negative for all variations. The magnitude of the Nusselt number decreases with increase in M and enhances at both the boundaries with increase in D^{-1} , $|\alpha|$ ($<0>$), Sc and $|S_0|$ ($<0>$). When the molecular buoyancy force dominates over the thermal buoyancy force $|Nu|$ enhances with N while it reduces at both the cylinders when they act in opposing directions. In general the Nusselt number on the inner cylinder is greater than that on the outer cylinder. In the case of TDS the Nusselt number on the inner cylinder is negative for all variations and positive on the outer cylinder. We find that $|Nu|$ enhances with increase in M, α and decreases with D^{-1} (tables.11,13,16,18). We find that $|Nu|$ reduces with N in both the cylinders when the forces act in the same direction and enhances on both cylinders with $|N|$ when they act in opposing directions. An increase in Sc enhances $|Nu|$ at the inner cylinder except at $G=10^3$ where it reduces with Sc while on the outer cylinder $|Nu|$ decreases with Sc . The behaviour of Nu with reference to S_0 shows that $|Nu|$ at both the cylinders depreciates with increase in $|S_0|$ ($<0>$). In the TDS case the Nusselt number at both the cylinders is exhibited in tables.40-50. It is found that the rate of heat transfer at the inner cylinder is negative and is positive at the outer cylinder for all variations in the parameters. The magnitude of Nu depreciates with M and D^{-1} and enhances with G and α . The variation of Nu with N shows that when the molecular force dominates over the thermal force $|Nu|$ at both the cylinders decrease with N when the forces act in the same direction and for the forces acting in opposite directions $|Nu|$ enhances with $|N|$ ($<0>$) at $r=1$ & 2 (tables.43,48). We infer that the rate of heat transfer decays with Sc for all G except for $G=1$ where $|Nu|$ increases with $Sc \leq 1.3$ and depreciates with $Sc \geq 2.01$ at $r=1$ & 2. In general we find that $|Nu|$ at the inner cylinder is less than that on the outer cylinder in both CS and TDS cases.

The Sherwood number (Sh) which measures the local rate of mass transfer on the boundaries has been depicted in tables for different values of G, D, N, M, N, Sc, S_0 and α . We find that the rate of mass transfer on the inner cylinder is positive and that on the outer cylinder is negative in both CS and TDS cases. In the VS case we find that the magnitude of Sh decreases with increase in M . The behaviour of Sh with D^{-1} shows that lesser the permeability of the porous medium greater the magnitude of Sh on the inner cylinder and smaller the magnitude of Sh on the outer cylinder. An increase in the strength of the heat source enhances $|Sh|$ at the inner cylinder and reduces it on the outer cylinder while reversed effect is noticed in the case of heat sink. $|Sh|$ depreciates on both the cylinders with increase in $|N|$ ($<0>$) irrespective of the directions of the buoyancy forces. We notice that lesser the molecular diffusivity larger the magnitude of the Sherwood number. Also $|Sh|$ enhances on either cylinders with increase in $|S_0|$ ($<0>$). In general $|Sh|$ on the inner cylinder is less than that on the outer cylinder. In the case TDS the rate of mass transfer on the inner cylinder is positive when the buoyancy forces act in the same directions and for positive variation of S_0 . It is negative when the forces act in different directions while the reversed effect is true in the outer cylinder. We find that $|Sh|$ on the inner cylinder decreases with increase in $|G|$ ($<0>$), M while on the outer cylinder $|Sh|$ enhances with G and decreases with M . An increase in the strength of the heat source depreciates $|Sh|$ on the inner cylinder and enhances it on the outer cylinder. Irrespective of the directions of the buoyancy forces $|Sh|$ reduces with increase in $|N|$ ($<0>$). An increase in $Sc \leq 0.6$ increases $|Sh|$ on the inner cylinder and reduces it on the outer cylinder and for $Sc \geq 1.3$, $|Sh|$ decreases on the inner cylinder and enhances on the outer cylinder. Thus lesser the molecular diffusivity larger the magnitude of Sh on the inner cylinder and smaller the magnitude of Sh on the outer cylinder and for further lowering of the molecular diffusivity we notice a depreciation in $|Sh|$ on the inner cylinder and an enhancement on the outer cylinder. Also the magnitude of $|Sh|$ enhances at both the boundaries with increase in $|S_0|$ ($<0>$). In general we find that $|Sh|$ on the inner cylinder is less than that on the outer cylinder.

Table.1
Nusselt Number(Nu) $r=1$
 $P=0.71, N=1, Sc=1.3, S_0=0.5$

G/τ	I	II	III	IV	V
10^3	-0.30746	-0.30891	-0.31061	-0.30171	-0.28920
3×10^3	-0.28535	-0.29440	-0.30510	-0.24927	-0.22726
5×10^3	-0.20629	-0.24254	-0.28539	1.53864	0.02633
-10^3	-0.30746	-0.30891	-0.31061	-0.30171	-0.28920

-3×10^3	-0.28535	-0.29440	-0.30510	-0.24927	-0.22726
-5×10^3	-0.20629	-0.24254	-0.28539	1.53864	0.02633

	I	II	III	IV	V
M	2	4	6	2	2
D^{-1}	10^3	10^3	10^3	3×10^3	5×10^3

Table.2
Nusselt Number(Nu) at $r=1$
 $P=0.71, M=2, D^{-1}=10^3$

G/τ	I	II	III
10^3	-0.30746	-1.20242	-1.88216
3×10^3	-0.28535	-1.18507	-1.86804
5×10^3	-0.20629	-1.12304	-1.81757
-10^3	-0.30746	-1.20242	-1.88216
-3×10^3	-0.28535	-1.18507	-1.86804
-5×10^3	-0.20629	-1.12304	-1.81757

	I	II	III
α	2	4	6

Table.3
Nusselt Number(Nu) at $r=1$
 $P=0.71, M=2, D^{-1}=10^3$

G/τ	I	II	III	IV
10^3	-0.307612	-0.30467	-0.30877	-0.31070
3×10^3	-0.28535	-0.26788	-0.30325	-0.30564
5×10^3	-0.20629	-0.13637	-0.27798	-0.28753
-10^3	-0.307612	-0.30467	-0.30877	-0.31070
-3×10^3	-0.28535	-0.26788	-0.30325	-0.30564
-5×10^3	-0.20629	-0.13637	-0.27798	-0.28753

	I	II	III	IV
N	1	2	-0.5	-0.8

Table.4
Nusselt Number(Nu) at $r=1$
 $P=0.71, M=2, D^{-1}=10^3$

G/τ	I	II	III	IV
10^3	-0.23177	-0.27936	-0.30467	-0.30492
3×10^3	-0.30213	-0.29738	-0.28535	-0.26940
5×10^3	-0.27347	-0.25443	-0.20629	-0.14248
-10^3	-0.23177	-0.27936	-0.30467	-0.30492
-3×10^3	-0.30213	-0.29738	-0.28535	-0.26940
-5×10^3	-0.27347	-0.25443	-0.20629	-0.14248

	I	II	III	IV
Sc	0.24	0.6	1.3	2.01

Table.5
Nusselt Number(Nu) at $r=1$
 $P=0.71, M=2, D^{-1}=10^3$

G/τ	I	II	III	IV
10^3	-0.30746	-0.30234	-0.31151	-0.31071
3×10^3	-0.28535	-0.25328	-0.31146	-0.30568
5×10^3	-0.20629	-0.07794	-0.31105	-0.28770
-10^3	-0.30746	-0.30234	-0.31151	-0.31071
-3×10^3	-0.28535	-0.25328	-0.31146	-0.30568
-5×10^3	-0.20629	-0.07794	-0.31105	-0.28770

	I	II	III	IV
S_0	0.5	1.0	-0.5	-1.0

Table.6
Nusselt Number(Nu) at the outer cylinder $r=2$
 $P=0.71, N=1, Sc=1.3, S_0=0.5$

G/τ	I	II	III	IV	V
10^3	1.53394	1.53495	1.53629	1.52910	1.52612
3×10^3	1.51543	1.52177	1.53014	1.48504	1.46638

5×10^3	1.44927	1.47464	1.50817	0.58744	1.25288
-10^3	1.53394	1.53495	1.53629	1.52910	1.52612
-3×10^3	1.51543	1.52177	1.53014	1.48504	1.46638
-5×10^3	1.44927	1.47464	1.50817	0.58744	1.25288

	I	II	III	IV	V
M	2	4	6	2	2
D^{-1}	10^3	10^3	10^3	3×10^3	5×10^3

Table.7
Nusselt Number(Nu) at $r=2$
 $P=0.71, M=2, D^{-1}=10^3$

G/τ	I	II	III
10^3	1.53394	2.57222	3.42277
3×10^3	1.51543	2.55665	3.40928
5×10^3	1.44927	2.50100	3.36108
-10^3	1.53394	2.57222	3.42277
-3×10^3	1.51543	2.55665	3.40928
-5×10^3	1.44927	2.50100	3.36108

	I	II	III
α	2	4	6

Table.8
Nusselt Number(Nu) at $r=2$
 $P=0.71, M=2, D^{-1}=10^3$

G/τ	I	II	III	IV
10^3	1.53394	1.53170	1.55012	1.53660
3×10^3	1.51543	1.50137	1.53006	1.53205
5×10^3	1.44927	1.39300	1.50780	1.51578
-10^3	1.53394	1.53170	1.55012	1.53660
-3×10^3	1.51543	1.50137	1.53006	1.53205
-5×10^3	1.44927	1.39300	1.50780	1.51578

	I	II	III	IV
N	1	2	-0.5	-0.8

Table.9
Nusselt Number(Nu) at $r=2$
 $P=0.71, M=2, D^{-1}=10^3$

G/τ	I	II	III	IV
10^3	1.19513	1.50919	1.53394	1.53173
3×10^3	1.52987	1.52581	1.51543	1.50155
5×10^3	1.50704	1.49080	1.44927	1.39371
-10^3	1.19513	1.50919	1.53394	1.53173
-3×10^3	1.52987	1.52581	1.51543	1.50155
-5×10^3	1.50704	1.49080	1.44927	1.39371

	I	II	III	IV
Sc	0.24	0.6	1.3	2.01

Table.10
Nusselt Number(Nu) at $r=2$
 $P=0.71, M=2, D^{-1}=10^3$

G/τ	I	II	III	IV
10^3	1.53394	1.52947	1.53737	1.53650
3×10^3	1.51543	1.48744	1.53637	1.53146
5×10^3	1.44927	1.33724	1.53627	1.51343
-10^3	1.53394	1.52947	1.53737	1.53650
-3×10^3	1.51543	1.48744	1.53637	1.53146
-5×10^3	1.44927	1.33724	1.53627	1.51343

	I	II	III	IV
S_0	0.5	1.0	-0.5	-1.0

Table.11
Sherwood Number(Sh) $r=1$
 $P=0.71, N=1, Sc=1.3, S_0=0.5$

G/τ	I	II	III	IV	V
----------	---	----	-----	----	---

10^3	10.32941	10.32846	10.32721	10.33375	10.33674
3×10^3	10.34675	10.34081	10.33297	10.37522	10.39270
5×10^3	10.40873	10.38495	10.35355	10.52275	10.59271
-10^3	10.32941	10.32846	10.32721	10.33375	10.33674
-3×10^3	10.34675	10.34081	10.33297	10.37522	10.39270
-5×10^3	10.40873	10.38495	10.35355	10.52275	10.59271

	I	II	III	IV	V
M	2	4	6	2	2
D^{-1}	10^3	10^3	10^3	3×10^3	5×10^3

Table.12
Sherwood Number(Sh) at $r=1$
 $P=0.71, M=2, D^{-1}=10^3$

G/τ	I	II	III
10^3	10.32941	6.23241	3.15036
3×10^3	10.34675	6.24699	3.16299
5×10^3	10.40873	6.29909	3.20811
-10^3	10.32941	6.23241	3.15036
-3×10^3	10.34675	6.24699	3.16299
-5×10^3	10.40873	6.29909	3.20811

	I	II	III
α	2	4	6

Table.13
Sherwood Number(Sh) at $r=1$
 $P=0.71, M=2, D^{-1}=10^3$

G/τ	I	II	III	IV
10^3	10.32941	5.91015	-16.16893	-9.53671
3×10^3	10.34675	5.93857	-16.16311	-9.53245
5×10^3	10.40873	6.04010	-16.14229	-9.51722
-10^3	10.32941	5.91015	-16.16893	-9.53671

-3×10^3	10.34675	5.93857	-16.16311	-9.53245
-5×10^3	10.40873	6.04010	-16.14229	-9.51722

	I	II	III	IV
N	1	2	-0.5	-0.8

Table.14

Sherwood Number(Sh) $r=1$
 $P=0.71, M=2, D^{-1}=10^3$

G/ τ	I	II	III	IV
10^3	17.65250	42.41882	10.32941	15.16402
3×10^3	3.11713	5.56950	10.34675	15.20772
5×10^3	3.12108	5.58465	10.40873	15.36388
-10^3	3.11603	5.56527	10.32941	15.16402
-3×10^3	3.11713	5.56950	10.34675	15.20772
-5×10^3	3.12108	5.58465	10.40873	15.36388

	I	II	III	IV
Sc	0.24	0.6	1.3	2.01

Table.15

Sherwood Number(Sh) at $r=1$
 $P=0.71, M=2, D^{-1}=10^3$

G/ τ	I	II	III	IV
10^3	10.23941	19.18409	-7.32681	-16.17192
3×10^3	10.34675	19.26281	-7.32687	-16.18133
5×10^3	10.40873	19.54409	-7.32704	-16.21500
-10^3	10.23941	19.18409	-7.32681	-16.17192
-3×10^3	10.34675	19.26281	-7.32687	-16.18133
-5×10^3	10.40873	19.54409	-7.32704	-16.21500

	I	II	III	IV
S_0	0.5	1.0	-0.5	-1.0

Table.16

Sherwood Number(Sh)at the outer cylinder $r=2$

$P=0.71$, $N=1$, $Sc=1.3$, $S_0=0.5$

G/τ	I	II	III	IV	V
10^3	-17.66180	-17.67222	-17.68549	-17.61527	-17.58681
3×10^3	-17.48322	-17.54859	-17.63202	-17.19139	-17.01315
5×10^3	-17.84496	-17.10676	-17.44083	-15.67629	-14.96256
-10^3	-17.66180	-17.67222	-17.68549	-17.61527	-17.58681
-3×10^3	-17.48322	-17.54859	-17.63202	-17.19139	-17.01315
-5×10^3	-17.84496	-17.10676	-17.44083	-15.67629	-14.96256

	I	II	III	IV	V
M	2	4	6	2	2
D^{-1}	10^3	10^3	10^3	3×10^3	5×10^3

Table.17

Sherwood Number(Sh) at $r=2$

$P=0.71$, $M=2$, $D^{-1}=10^3$

G/τ	I	II	III
10^3	-17.66180	-20.52195	-22.56638
3×10^3	-17.48322	-20.37939	-22.44850
5×10^3	-17.84496	-19.86985	-22.02711
-10^3	-17.66180	-20.52195	-22.56638
-3×10^3	-17.48322	-20.37939	-22.44850
-5×10^3	-17.84496	-19.86985	-22.02711

	I	II	III
α	2	4	6

Table.18

Sherwood Number(Sh)at $r=2$

$P=0.71$, $M=2$, $D^{-1}=10^3$

G/τ	I	II	III	IV
10^3	-17.66180	-8.92132	34.61112	21.52908
3×10^3	-17.48322	-8.63063	34.67238	21.57421

5×10^3	-16.84496	-7.59162	34.89141	21.73559
-10^3	-17.66180	-8.92132	34.61112	21.52908
-3×10^3	-17.48322	-8.63063	34.67238	21.57421
-5×10^3	-16.84496	-7.59162	34.89141	21.73559

	I	II	III	IV
N	1	2	-0.5	-0.8

Table.19
Sherwood Number(Sh)at $r=2$
 $P=0.71, M=2, D^{-1}=10^3$

G/τ	I	II	III	IV
10^3	-25.90158	-21.45485	-17.66180	-27.13415
3×10^3	-3.46264	-8.25404	-17.48322	-26.68006
5×10^3	-3.42316	-8.10056	-16.84496	-25.05739
-10^3	-3.47367	-8.29695	-17.66180	-27.13415
-3×10^3	-3.46264	-8.25404	-17.48322	-26.68006
-5×10^3	-3.42316	-8.10056	-16.84496	-25.05739

	I	II	III	IV
Sc	0.24	0.6	1.3	2.01

Table.20
Sherwood Number(Sh)at $r=2$
 $P=0.71, M=2, D^{-1}=10^3$

G/τ	I	II	III	IV
10^3	-17.66180	-34.97915	17.16215	34.58264
3×10^3	-17.48322	-34.15703	17.16216	34.47394
5×10^3	-16.84495	-31.21948	17.16115	34.08517
-10^3	-17.66180	-34.97915	17.16215	34.58264
-3×10^3	-17.48322	-34.15703	17.16216	34.47394
-5×10^3	-16.84495	-31.21948	17.16115	34.08517

	I	II	III	IV
--	---	----	-----	----

S_0	0.5	1.0	-0.5	-1.0
-------	-----	-----	------	------

6. References

1. Al-Nimr.M.A : Analytical solution for transient laminar fully developed free convection in vertical annuli. Int.J.Heat and mass transfer, V.36, PP 2388-2395, (1993)
2. Antonio Barletle : Combined forced and free convection with viscous dissipation in a vertical duct. Int.J.Heat and mass transfer, V.42, PP 2243-2253, (1999)
3. Caltagirone.J.P : J.Fluid. Mech, vol.76, P 337, (1976)
4. Chen.T.S and Yuh.C.F : Combined heat and mass transfer in natural convection on inclined surface. J. Heat transfer, V.2, PP 233-250, (1979)
5. Faces.N and Farouq.B : ASME, J. Heat transfer, V.105, P 680, (1983)
6. Ganapathy.R and Purusotham.R : Fluid flow induced by a traveling transverse wave in a saturated porous medium. J.Ind.Inst.Sci, V.70, PP 333-340, (1990)
7. Havstad.M.A and Burns.P.J : Int.J.Heat and mass transfer, V.25, No.1, P 1755, (1982)
8. Mihersen and Torrance.K.E : Int.J.Heat and mass transfer, V.30, No.4, P 729, (1987)
9. Nanda.R.S and Purushotham.R : Int. dedication seminar on recent advances on maths and applications, Varanasi, (1976)
10. Neeraja.G : Ph.D thesis, S.P.Mahila University, Tirupathi, India, (1993)
11. Nguyen.T.H, Satish.M.G, Robillard.L and Vasseur.P : ASME, The American Society of Mechanical Engineers, Paper No 85-WA/HT-8, Newyork, (1985)
12. Osterle.J.F and Young.F.J : J.Fluid Mechanics, Vol.11, P 512, (1961)
13. Philip.J.R : Axisymmetric free convection at small Rayleigh numbers in porous cavities. Int.J.Heat and mass transfer, V.25, PP 1689-1699, (1982)
14. Poots.G : Int.J.Heat and mass transfer, Vol.3, P 1, (1961)
15. Prasad.V : Natural convection in porous media. Ph.D thesis, S.K.University, Anantapur, India, (1983)
16. Prasad.V and Kulacki.F.A : Int.J.Heat and mass transfer, Vol.27, P 207, (1984)
17. Prasad.V, Kulacki.F.A and Keyhari.M : J.Fluid.Mech, Vol 150, P 89, (1985)
18. Prasad.R.M.V : Hydromagnetic convective heat and mass transfer through a porous medium in channels/pipes. Ph.D thesis, S.K.University, Anantapur, India, (2006)
19. Rani : Unsteady convective heat and mass transfer flow through a porous medium in wavy channels. Ph.D thesis, S.K.University, Anantapur, India, (2003)
20. Rao.Y.F, Miki.Y, Fukuda takata.Y and Hasegahea.S : Int.J.Heat and mass transfer, Vol.28, P 705, (1985)
21. Robillard.L, Ngugen.T.H, Satish.M.G and Vasseur.P : Heat transfer in porous media and particulate flows, HTD-V.46, P 41, ASME, (1985)
22. Sastri.V.U.K and Bhadrani.C.V.V : App. Sci. Res, Vol.34, 2/3, P 117, (1978)
23. Shaarawi.El.M.A.I and Al – Nimr.M.A : Fully developed laminar natural convection in open ended vertical concentric annuli. Int.J.Heat and mass transfer, PP 1873-1884, (1990)
24. Singh.K.R and Cowling.T.J : Q. J. Maths. Appl. Maths, Vol 16, P 1, (1963)
25. Sivanjaneya Prasad : Effects of convection heat and mass transfer in unsteady hydromagnetic channels flow. Ph.D thesis, S.K.University, Anantapur, India, (2001)
26. Sreenivas Reddy : Thermo diffusion effect on convective heat and mass transfer through a porous medium. Ph.D thesis, S.K.University, Anantapur, India, (2006)
27. Sreevani.M : Mixed convection heat and mass transfer through a porous medium in channels with dissipative effects. Ph.D thesis, S.K.University, Anantapur, India, (2003)
28. Vassuer.P, Nguyen.T.H, Robillard and Thi.V.K.T : Int.J.Heat and mass transfer, Vol.27, P 337, (1984)
29. White head.J.A : Observations of rapid means flow produced in mercury by a moving heater, Geo phys.Fluid dynamics, Vol.3, PP 161-180, (1972)
30. Yu.C.P : Appl.Sci.Res. Vol 22, P 127, (1970)
31. Yu.C.P and Yong.H : Appl.Sci.Res, Vol 20, P 16, (1969)